Physics – Uspekhi **51** (1) 79 – 100 (2008)

INSTRUMENTS AND METHODS OF INVESTIGATION

PACS numbers: **52.80. – s**, **84.70. + p**, **85.45. – w**

Electron emission from ferroelectric plasma cathodes

G A Mesyats

DOI: 10.1070/PU2008v051n01ABEH006426

Contents

Abstract. Recent and not so recent experimental data are analyzed to show that the reason for strong electron emission from dielectric cathodes is the incomplete discharge occurring on the dielectric surface due to the electric field there being tangentially nonzero. The places of origin of such discharges are the metal – dielectric – vacuum triple junctions (TJs). As the discharge plasma moves over the surface of the dielectric electrode, the bias current arises, and an electric microexplosion occurs at a TJ. If the number of TJs is large, as it is for a metal grid held tightly to a ferroelectric, electron currents of up to 10^4 A with densities of more than 10^2 A cm^{-2} can be achieved. A surface discharge is initiated by applying a triggering pulse to the metal substrate deposited beforehand onto the opposite side of the ferroelectric. If this pulse leads the accelerating voltage pulse, the electron current is many times the Child – Langmuir current. The reason for the ferroelectric effect is the large permittivity ($\varepsilon > 10^3$) of the materials used ($BaTiO_3$, PLZT, PZT). Although these devices have come to be known as ferroelectric cathodes, we believe ferroelectric plasma cathodes would be a better term to use to emphasize the key role of plasma effects.

G A Mesyats P N Lebedev Physical Institute,
Russian Academy of Sciences,
Leninskii prosp. 53, 119991 Moscow, Russian Federation
Tel. (7-499) 135 24 30. Fax (7-495) 956 24 04
E-mail: mesyats@pran.ru, mesyats@sci.lebedev.ru

Received 28 June 2007, revised 14 August 2007
Uspekhi Fizicheskikh Nauk **178** (1) 85 – 108 (2008)
DOI: 10.3367/UFNr.0178.200801e.0085
Translated by E G Strel'chenko; edited by A Radzig

1. Introduction

Producing high-current pulsed beams requires electron accelerators, whose two key elements are an electron-accelerating diode and a generator of accelerating voltage pulses [1]. The diodes of high-power pulsed accelerators with a current of up to 10^6 A commonly use explosive electron emission (EEE) cathodes [1] with energies between several hundred keV and several megaelectron-volts and durations from 10^{-10} to 10^{-7} s as electron sources. To produce electron beams of $10^3 - 10^5$ eV in energy, $10 - 10^3$ A in current, and 10^2 A cm^{-2} or more in current density, ferroelectric plasma (FEP) cathodes are employed. In these, plasma forms at places where the ferroelectric and the metal are in contact with each other. Electron beam parameters such as electron energy, current, perveance, diode triggering instant, aperture and so forth are easy to control in accelerators with FEP cathodes. Electron beam pulses in the diodes based on FEP cathodes generally last between 10^{-8} and 10^{-6} s, and occasionally for as long as 10^{-3} s. Such cathodes provide a good alternative to thermionic ones, whose current density does not exceed 10 A cm^{-2}, and compared to which they are cheaper and much easier to operate.

The idea of inventing a dielectric cathode emerged from the study in Refs [2, 3] on a discharge over the surface of a dielectric at the contact between the cathode and the forsterite or steatite ceramics. What the study showed was that in the incomplete discharge regime, owing to the high tangential component of an electric field at the ceramics – cathode contact — which was termed a triple junction, or a TJ (metal – dielectric – vacuum) — electron currents of up to 100 A can be derived from this contact. However, it is only when $BaTiO_3$, ferroelectric barium titanate, was taken as the dielectric that the performance of the cathode was radically

improved. To achieve a large current amplitude and to make the beam uniform over the cross section, it was proposed [4] that a metal grid or a ring-washer be mounted on one side of the cylindrical $BaTiO_3$ disk. At the places where the grid and $BaTiO_3$ are in contact, a large number of TJs form. The ring-washer (or the grid) were usually grounded, and the other side of the disk was coated with a metal film to which a triggering pulse was applied. As a result, a plasma coating formed at the surface of the ferroelectric, leading to electron emission. In 1967, a 50-keV, 2-kA, 100-ns electron beam was for the first time obtained from a diode with such a cathode by the present author and his coworkers at the Tomsk Polytechnical Institute.

Over the last two decades there has been a large increase in interest in such cathodes (for a review and references cited therein see Ref. [6]). It is hypothesized that what causes the emission effect in question is actually the release of electrons directly from the surface of the ferroelectric and not, as earlier thought [2 – 5], from the grid metal (in a plasma-assisted manner). Such cathodes have even been called ferroelectric (as has the emission itself, leading to the term 'ferroemission' [6]) — all this referring to precisely the same cathode design as described in Refs [4, 5]. A key result from the series of works reviewed in Ref. [6] is that applying about a 1-kV triggering pulse to a ferroelectric whose back and front surfaces are coated with metal and a grid (or strip) electrode, respectively, produces a strong electron emission from the cathode's front surface.

In the remainder of this Introduction we briefly outline the theoretical assumptions reviewed in Ref. [6], postponing their detailed analysis to Section 4.4.

The most popular model of electron ferroemission relies on the ability of a ferroelectric to change its polarization when exposed to a high-voltage pulse [7 – 9]. It is believed that rapid domain repolarization (within a few nanoseconds) within a ferroelectric sample induces a very strong electric field (up to 10^9 V cm^{-1}) close to the surface: the low conductivity of the ferroelectric prevents the rapid redistribution of 'free charges' capable of compensating for the domain's 'bound' charge due to nonequilibrium repolarization. As a result, an uncompensated negative charge forms near the surface of the ferroelectric, thus producing a strong electric field that gives rise to marked field emission from the ferroelectric surface [7].

This model is not without its challenges, though. First, there is still a question mark about whether the ferroelectric can indeed be rapidly repolarized. Experiments show that nanosecond repolarization occurs only in submicron ferroelectric films under the action of an electric field of $(2-4) \times 10^4$ V cm^{-1}, a fact that agrees well with theoretical predictions [10]. There is, however, experimental evidence of strong electron emission from 0.2- to 2.0-mm-thick ferroelectric films in electric fields of $\sim (2-3) \times 10^4$ V cm^{-1} [7, 11] — fields for which the expected repolarization time is much longer than a few nanoseconds [12]. Mention should also be made of a recent study of how domain repolarization depends on the average size of grains [13]; it has been found that a decrease in average grain size from 7 to 1 μm reduces catastrophically the fraction of domains capable of repolarizing during the period of time the inverse voltage is applied (60 kV cm^{-1} at a temperature of 100 °C for 30 min). A further weakness of the model is the presence of a strong tangential electric field which at a strength of $\sim 10^4 - 10^5$ V cm^{-1} gives rise to a surface charge [1]. It is well known that a surface discharge leads to the formation of plasma which supplies charges needed for the unscreened charges to be compensated; in other words, the surface plasma prevents the electric field from increasing further. Importantly, calculations in Refs [11, 14] predict the presence of strong tangential electric fields capable of producing a surface discharge on a ferroelectric sample — which is exactly the surface discharge observed earlier [2, 3].

The model of electron ferroemission is also at odds with experiments [15] on PLZT (lead – lanthanum – zirconium – titanium) ceramics, a material that has two different nonferromagnetic phases, one antiferroelectric and the other paraelectric. In these experiments, the back electrode was subjected to uni- or bipolar high-voltage (HV) pulses. Electron emission from a nonpolar ferroelectric PLZT sample was also evidenced in Ref. [16]. Polar PZT (lead – zirconium – titanium) samples were observed to display electron emission at twice the Curie temperature [17]. In Ref. [18], it was shown that if a back electrode of a nonpolar PZT sample is subjected to a positive or negative HV pulse, then ion emission is present along with electron emission — clearly direct experimental evidence of the plasma formation at the surface of a ferroelectric sample.

Experiments with triglycinesulfate (TGS) crystals [19, 20] and those with PLZT samples have provided yet more evidence that an HV pulse applied to a sample produces plasma. In Ref. [16], it is conjectured that the plasma forms at the ferroelectric surface. For evidence of this see also Refs [21 – 23].

The aim of this paper is to highlight the dominant role of plasma effects in how ferroelectric-based cathodes work. Ferroelectric effects (setting aside the fundamental role of the high permittivity, $\varepsilon > 10^3$) can be of significance at relatively small triggering pulses for which emission current densities are not ultimately high (see Section 4.4); in other words, the ferroelectric effects are important in situations that are of no relevance to applied high-current electronics. This paper begins by considering an incomplete pulsed discharge over the surface of a dielectric in a vacuum — the situation which first led the author to the idea of an FEP cathode [2, 4, 5]. This is followed by a discussion of triple junction effects for a case where special point cathodes are employed. The paper then describes the operation of high-current electron diodes with such cathodes and discusses their high-current electronics applications.

2. Pulsed discharge over the surface of a dielectric in a vacuum

2.1 Prebreakdown current

Let us briefly summarize electron emission results for an incomplete discharge over the surface of ceramics under the conditions of a grossly nonuniform cathode field [2, 3]. The electrodes and dielectric are arranged as shown in Fig. 1a. The cathode has the shape of a pin, a sharp-edged cylinder of diameter $D_c \ll D_d$, where D_d is the diameter of the dielectric cylinder. Occasionally, a truncated cylinder or a cone inclined at an angle α to the anode's surface normal (Fig. 1a) was used as the dielectric.

The flat anode of diameter D_a had its edges rounded. The cathode face, where the discharge took place, had a length $l = (D_a - D_c)/2$. The cathode – anode gap was subjected to a rectangular pulse of 500 ns duration (with ~ 1 ns pulse rise

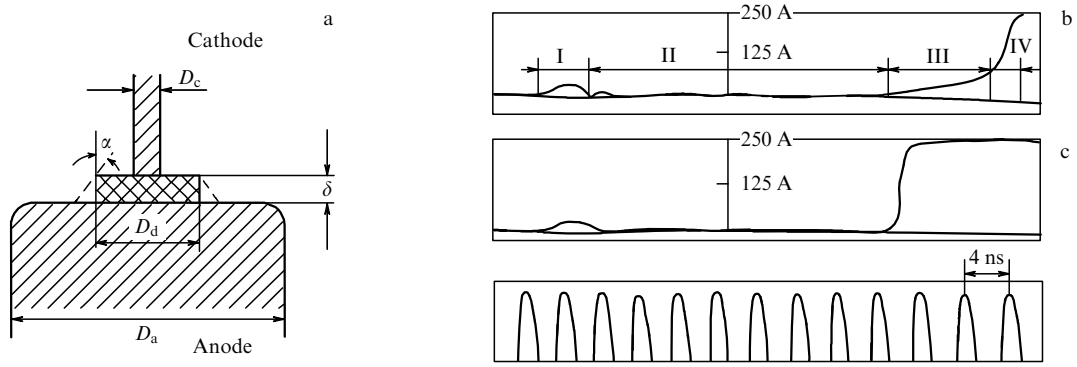

Figure 1. Study of a discharge over a steatite ceramics surface in a vacuum. (a) Electrode configurations: δ, thickness of a dielectric; D_c, D_d, D_a, the cylinder diameters of the cathode, dielectric, and anode; shaded segments indicate a truncated conical dielectric. Typical discharge current oscillograms are as follows: (b) for $D_a > D_d$, $\delta = 2$ mm, $D_d = 11$ mm, $D_c = 5$ mm, $D_a = 22$ mm, $U = 35$ kV, and (c) $D_a = D_d = 11$ mm.

time) and $\leqslant 50$ kV amplitude. Figure 1b shows current oscillograms for a discharge over steatite ceramics, in each of which four characteristic regions (I–IV) are recognized. The first is a peak due to the bias current through the dielectric, resulting from the rapid increase in the electric field during the pulse rise time. The second region is one of a relatively low (of order 1 A) current. In the third region one can see a considerable (up to ~ 100 A) increase in current. Finally, in the fourth region the current increases rapidly (within $\leqslant 1$ ns) to the magnitude limited by the line wave impedance and the voltage pulse amplitude.

The current in region III is of most interest for us here. It decreases with decreasing the ratio D_a/D_d, and for $D_a/D_d \leqslant 1$ regions II and III merge (Fig. 1c). For $D_a/D_d > 1$, region III shows a strong increase in current with increasing dielectric thickness, as well as in the presence of anode indentation under the dielectric. Electron-optical studies of the breakdown process on the surface of forsterite ceramics showed that plasma at the cathode–dielectric contact starts to glow within the first 3 ns. The glow moves toward the anode at about 10^7 cm s^{-1} and after reaching the edge of the ceramics starts to move toward the anode at about 10^8 cm s^{-1}. The instant of time when the glow first appears on the anode face of the truncated conical dielectric depends on the angle α the face makes with the anode normal. At $\alpha = 0$ (cylindrical dielectric), glow on the anode face was only seen after the plasma from the cathode reached the upper edge of the dielectric's anode face. For $\alpha = 10°$, the anode face is seen to glow even in region III, when the plasma has not yet reached this face. When the plasma arrives at the anode, a sharp flash occurs and a cathode spot and an anode spot appear on either electrode.

The results above were considered to imply that the current in region III is due to the electrons arriving at the anode before the plasma reaches the anode face — that is, in the incomplete discharge regime [2, 3]. Supporting this view is the fact that increasing the anode diameter D_a — and thus allowing more electrons from the cathode to reach the anode — results in a much higher current in region III. Additional supporting evidence is that the anode face shows a glow at an inclination angle of $\alpha = 10°$ before being reached by the plasma from the cathode. This glow is due to a discharge which occurs over the surface of the anode face and is initiated by those electrons from region III that arrive at this face. At $\alpha = 0$, the possibility of landing at the anode face is eliminated and it shows no glow before the plasma from the cathode comes. In further support of this, note that the current in region III increases if there is an indentation at the anode or if the thickness of the dielectric increases, i.e., when the electric field component normal to the surface of the dielectric decreases. Measurements using ultrahigh-speed electron-optical photography [2, 3] showed that the cathode plasma moves along the dielectric surface with a velocity approximately proportional to the cathode–anode potential difference U. In absolute values, the velocity of the plasma along the dielectric surface was $(1-3) \times 10^7$ cm s^{-1} [3] for a dielectric thickness of $\delta = 2$ mm.

With a pin as the anode, plasma appeared both in the near-cathode and near-anode regions. As time elapses, the two plasma streams start moving toward each other. At the instant they meet, both the cathode and anode faces produce an intense flash of light, and on the cathode and the anode there appear a cathode spot and an anode spot — indicating the onset of an arc discharge.

2.2 Effect of a discharge voltage decrease in the pulsed regime

For a nonuniform field at the cathode and a cathode diameter smaller than that of the dielectric, the pulsed voltage U at which the discharge arises over a dielectric in a vacuum is found to be greatly reduced from the static value U_{st}. The reason for this is that the tangential field component near the cathode gains as a result of the potential being distributed unevenly over the dielectric surface due to the presence of surface and volumetric capacitances. The tangential (E_t) and normal (E_n) field components at the surface of the dielectric at a distance x from the cathode surface are given, for $l \gg D_c$ and assuming the voltage drop to be ideal, by the expressions [3, 23]

$$E_t(x) = U\gamma \frac{\cosh \gamma(l-x)}{\sinh \gamma l}, \quad (1)$$

$$E_n(x) = \frac{U}{\delta} \frac{\sinh \gamma(l-x)}{\sinh \gamma l}, \quad (2)$$

where

$$\gamma = \left(\frac{pC_1 + \sigma_1}{pC_2 + \sigma_2}\right)^{1/2}, \quad (3)$$

δ is the thickness of the dielectric, x is the distance from the surface of the cathode to the point of consideration at the

surface of the dielectric, l is the length of the dielectric, p is the Laplace transform operator used in electric circuit transient analysis, $C_1 = \varepsilon\varepsilon_0/\delta$ is the capacitance [F cm^{-2}] of a unit area of the dielectric surface relative to the lower electrode, $C_2 = k\varepsilon_0$ is the specific mutual capacitance of dielectric surface unit areas, k is a constant dependent on the properties of the dielectric surface, σ_1 is the bulk conductivity [$(\Omega\ \mathrm{cm}^2)^{-1}$], σ_2 is the surface conductivity [Ω^{-1}], and U is the applied voltage [V].

Because the time $t \sim p^{-1}$, it follows from formulas (1) and (2) that if the characteristic voltage application time $t \gg C_1/\sigma_1$ and $t \gg C_2/\sigma_2$, then $\gamma = (\sigma_1/\sigma_2)^{1/2}$, and that if $t \ll C_1/\sigma_1$ and $t \ll C_2/\sigma_2$, then $\gamma = (C_1/C_2)^{1/2}$, the former and the latter results corresponding to the pulsed breakdown and static breakdown, respectively. If $r \ll x \ll l$, where r is the rounding-off radius of the dielectric-adjacent cathode, then the tangential and normal field components are given by the respective expressions

$$E_\mathrm{t} = \frac{E_\mathrm{ot}\gamma l}{\tanh \gamma l}\,, \qquad E_\mathrm{n} = \frac{U}{\delta}\,, \tag{4}$$

where $E_\mathrm{ot} = U/l$ is the average tangential field at the surface of the dielectric.

If in the stationary regime $\gamma l < 0.5$ and in the pulsed regime $\gamma l \geqslant 1$, then for the stationary case $E_\mathrm{t} \approx U/l$, and for the pulsed case $E_\mathrm{t} = U\gamma/\tanh \gamma l$, indicating that the increase in the pulsed, compared to the stationary, field corresponds to the condition $\gamma l/\tanh \gamma l > 1$. For $\gamma l > 2$, the field increase factor in the pulsed regime is $\sim l(\varepsilon/\delta)^{1/2}$. Hence, the thinner and longer the dielectric and the higher the dielectric constant, the lower the amplitude ratio of a pulsed discharge voltage in a vacuum to the static discharge voltage — a very important conclusion as far as the operation of ferroelectric plasma cathodes (for which $\varepsilon \geqslant 10^3$) is concerned (noting the low voltage amplitude of the cathode control pulse used).

2.3 Cathode – dielectric contact processes

The presence of a dielectric in the vacuum gap leads to strengthening the electric field in the region of the cathode – dielectric contact due to microgaps. Processes occurring in a metal – dielectric contact subjected to an electric field were explored in Ref. [25]. In this contact, electrons, due to the increased electric field, appeared before the vacuum breakdown. The electrodes and insulator were placed in a magnetic field oriented perpendicular to the electric field in order to remove electrons from the discharge gap. Grounded phosphor-coated plates were used as 'electron dumps'.

The interelectrode voltage needed for the phosphor to start glowing provides a criterion against which the intensity of contact phenomena can be judged. As the dielectric constant increased, more electrons left the contact — with the result that the pulsed voltage producing the cathode glow reduced about sevenfold when the dielectric constant ε of the dielectric was increased from 6.6 (steatite) to 1800 (barium titanate) (Table 1).

The electron current can also be enhanced by increasing the electric field strength in the contact area via changing the shape of the cathode (replacing a flat cathode by a pointed one). Changing the material of the cathode has little effect on electron escape from the contact.

The reason for the increased field strength in the region of the cathode – dielectric contact is that neither the dielectric nor the cathode can have perfectly smooth surfaces and the only way they touch each other is through the protrusions

Table 1. Pulsed voltage and field strength values corresponding to the instant of appearance of a glow at the cathode – dielectric contact for different dielectrics [25].

Dielectric	ε	Voltage on the dielectric, kV	Field strength in the gap (0.025 mm), kV cm^{-1}
Steatite	6.6	21.5	120
Zirconium porcelain	9.5	25.0	200
Rutile	8.0	8.3	480
Barium titanate	1800	3.3	1300

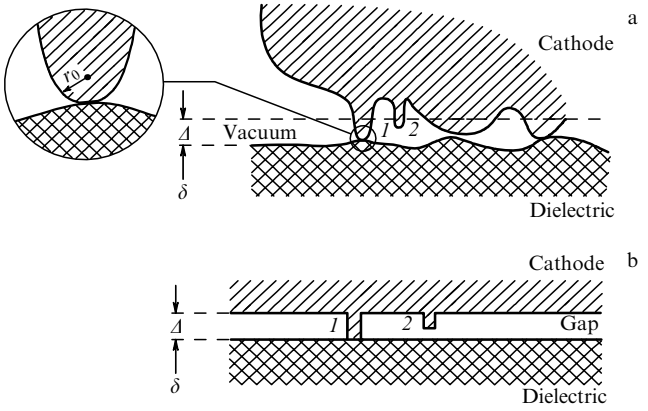

Figure 2. (a) Shape of the dielectric – cathode contact: r_0, rounding-off radius of the cathode surface protrusion; Δ, average cathode – dielectric gap width; δ, dielectric thickness; *1*, tip in contact; *2*, tip with no contact. (b) Stylized picture of the cathode – dielectric contact.

they have (Fig. 2a). The electric field strength in the contact region can be approximately estimated using a somewhat idealized form of the cathode geometry (Fig. 2b). Let us denote by Δ the averaged width of the microgap in the cathode – dielectric contact, and by δ the thickness of the dielectric. Assuming that the gap is much wider than it is long, the electric field within it can be considered uniform everywhere except at its edges. The field strength E_c in the cathode gap can be determined as the field strength in the gap connected in series with the dielectric:

$$E_\mathrm{c} = \frac{U/\Delta}{1 + \delta/\varepsilon\Delta}\,, \tag{5}$$

where E_c is the electric field strength in the cathode region. From this relationship, two things follow. First, if $\delta/\varepsilon\Delta \ll 1$, then

$$E_\mathrm{c} \approx \frac{U}{\Delta} = E\,\frac{\delta}{\Delta}\,, \tag{6}$$

where $E = U/\delta$ is the average electric field in the dielectric gap. Thus, in this case the electric field in the gap increases by a factor of δ/Δ. Second, if $\delta/\varepsilon\Delta \gg 1$, then

$$E_\mathrm{c} \approx \varepsilon E\,, \tag{7}$$

i.e., the electric field strength increases by a factor of ε.

However, the electric field at the cathode micropoints will be still greater due to the geometric enhancement effect [24]. Denoting the micropoint height by h and the radius of the cathode point tip by r_0, it is found for $h < \Delta$ that

$$E_\mathrm{c0} \approx \frac{E_\mathrm{c} h}{r_0} = \beta E_\mathrm{c}\,, \tag{8}$$

where β is the electric field amplification factor. In particular, this is exactly the field amplification observed for point tip *2* for the case illustrated in Fig. 2a. The factor β can be as large as 10 to 100 [23], implying that the full field amplification for large ε is of order $\delta h/\Delta r_0$. If $\delta = 1$ cm, $\Delta = 10^{-3}$ cm, $h = 10^{-4}$ cm, $r_0 = 10^{-5}$ cm, and the voltage $U = 10^4$ V, then the electric field strength at the surface of the point (for example, point *2* in Fig. 2) reaches 10^8 V cm^{-1}. Such a point tip explodes within $\sim 10^{-9}$ s due to the presence of an field emission current [1]. (For more on that see Section 3.1.)

The plasma and electron beam in this scenario reach the dielectric and also lead to a surface discharge [1, 24], so that, independent of whether or not the point tip touches the dielectric surface, we will call either case a triple junction (TJ). We will, though, classify triple junctions into type 1 for the touch case, and type 2 for the case with no touch.

3. Research on emission processes in point-cathode diodes

3.1 Explosive electron emission

Before proceeding to electron emission from a metal–dielectric–vacuum TJ, we will briefly present the fundamentals of explosive electron emission (EEE) from metal tips — a process which we believe is of great relevance to the cathodes of interest here. Explosive electron emission represents electron emission resulting from microscopic explosions that occur on the surface of a metal or graphite cathode due to the high concentration of energy in surface microvolumes [2, 26]. The reasons for an explosion of a metal microvolume and EEE initiation vary from an accelerated microparticle hitting the cathode to a laser pulse focused on the cathode, and to an ion or neutral-particle or plasma beam striking it [27]. However, the simplest and most widespread approach to initiating EEE is to rapidly heat microregions of the cathode by the Joule heat due to the high current density of field emission (FE).

To achieve a high FE current density, a strong electric field is needed. Such a field can be produced by using metal micropoints as cathodes. Moreover, any flat metal cathode has surface microprotrusions, whereon electric field increases by a factor of β compared to the average electric field between the cathode and anode equal to $E_0 = U/d$, where U is the voltage, and d is the electrode spacing. According to the Fowler–Nordheim formula, the FE current density j depends as follows on the field strength on the tip of a protrusion [28]:

$$j = \frac{1.55 \times 10^{-6} E^2}{\varphi} \exp\left(-\frac{6.85 \times 10^7 \varphi^{3/2}}{E}\right), \tag{9}$$

where φ is the work function of the cathode metal (in eV), and the electric field strength E is measured in units of V cm^{-1}.

If the electric field at the tip of a micropoint is $E = 10^8$ V cm^{-1}, then the FE current density is as high as $j = 10^9$ A cm^{-2} [1]. At this large a value of j the tip explodes after a span of time $t_d \approx 10^{-9}$ s. This length of time, known as the explosion delay time, can be estimated from the relation [1, 26]

$$j^2 t_d = \bar{h}, \tag{10}$$

where $\bar{h}$, the specific action for the explosion of the metal, is of order 10^9 A^2 s cm^{-4} for most metals [27].

A feature of EEE is that the cathode emits electrons in short-duration portions ($10^{-9}-10^{-8}$ s) of an avalanche nature, each with $10^{11}-10^{12}$ electrons in it. We named such electron avalanches the ectons [29]. The question now arises: why do such portions form, or why does the current cut off? The picture of a current cutoff is as follows. As an ecton first emerges, FE current density of as much as 10^9 A cm^{-2} occurs, with the result that a microvolume on the cathode surface is rapidly heated and subsequently explodes, leading to intense thermal electron emission due to the metal being overheated. As the explosion develops, a variety of processes occurs, including the enlargement of the electron emission zone, heat removal, and energy removal due to the evaporation and ejection of the heated liquid metal. All of this cools the electron emission zone and decreases the FE current density, thus leading to a still faster cooling of the emission zone due to the decreased Joule heating temperature.

The microprotrusions we are considering can exist on any flat metal surface but can also be created intentionally, as exemplified by microtip cathodes and those formed by a set of blades or foils, metal or graphite felt. Much experimental evidence suggests, however, that such cathodes are rather short-lived due to factors such as mass removal, microprotrusion melting, and the curling up of emitting edges. Moreover, with such cathodes it is usually difficult to produce uniform electron beams with large cross sections. A beam will be uniform if the cathode surface is filled uniformly by the plasma from the microexplosions occurring at the cathode. There are a number of factors, however — such as the low velocity of the cathode plasma and random and not simultaneous tip explosions (due to screening and stroke effects, the electron field difference between microprotrusion tips, etc.) [1] — which usually hinder the uniform distribution of the electron current density and, most important, do not allow making this distribution pulse-to-pulse stable. For the diode comprising a pointed cathode and flat anode, the EEE current for the case of nonrelativistic electrons in given by the expression [24]

$$i = A_1 U^{3/2} \frac{vt}{d - vt}, \tag{11}$$

where $A_1 \approx 37 \times 10^{-6}$ A V$^{-3/2}$, v is the cathode plasma expansion velocity, U is the voltage, d is the cathode–anode gap length, and t is the time. The velocity is typically $v \sim 10^6$ cm s^{-1} [2, 24]. If there are many tips with a characteristic intertip separation of far less than d, which explode in a time less than the pulse rise time, then the EEE current in the diode is found from the relationship

$$i = A_2 U^{3/2} \frac{S}{(d - vt)^2}, \tag{12}$$

where S is the cathode area, and $A_2 = 2.3 \times 10^{-6}$ A V$^{-3/2}$.

One of the standout features of EEE is the so-called double pulse effect [26] in which, if two identical voltage pulses are applied to a diode at a time interval of τ_d, the electron current i_2 in the second pulse will be many times the current i_1 in the first. As Fig. 3 suggests, in the case of a point cathode and flat anode the ratio i_1/i_2 can be as large as 10 [30]. For lengths of $d \sim 1$ mm, pulse durations of 10^{-8} s, and voltages of $\sim 10^4$ V this effect disappears at $\tau_d \sim 10^{-7}$ s. The effect is due to the fact that the diode gap is partially filled by the plasma resulting from the microexplosion the first pulse triggers at the cathode. The role of the plasma produced by

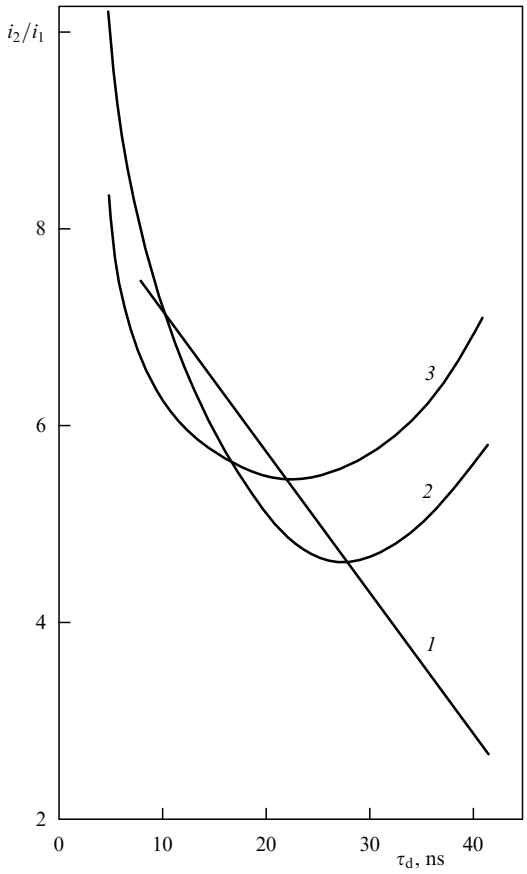

Figure 3. Current ratio i_2/i_1 as a function of interpulse time interval τ_d for $U = 13.5$ kV (*1*), $U = 20$ kV (*2*), and $U = 28$ kV (*3*).

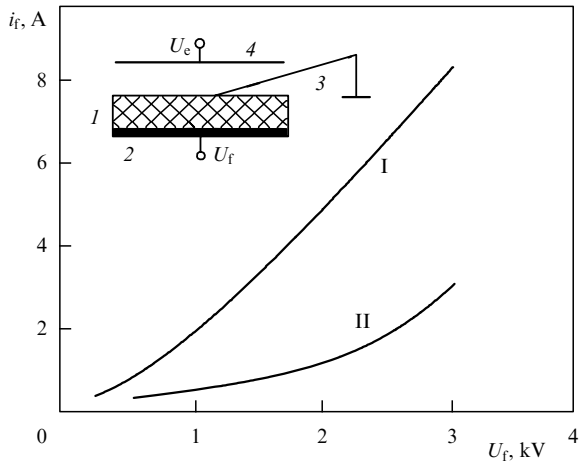

Figure 4. Discharge current i_f over the surface of a $BaTiO_3$ ferroelectric ($\delta = 2$ mm) versus the amplitude U_f of the voltage pulse between needle *3* and substrate *2*. Upper inset: *1*, dielectric; *4*, diode anode. Line I was obtained for the case in which electrode *3* served as cathode with respect to substrate *2*, while line II corresponded to the case where electrode *3* served as anode.

the first pulse increases still further if this pulse acts long enough that the beam of accelerated EEE electrons heating the anode has time to produce anode plasma — a situation which occurs for relatively high diode voltages and a closely spaced cathode and anode. It is this which explains the minimum in i_2/i_1 as a function of τ_d in Fig. 3.

As already mentioned above, EEE electron beams are fundamentally nonuniform because the pulsed voltage that accelerates electrons also triggers cathode microexplosions due to the FE current. Therefore, one of the fundamental approaches to making the beam electron distribution uniform is to separate the function of accelerating electrons from that of triggering cathode microexplosions. This necessitates utilizing metal – dielectric cathodes that depend for their operation on phenomena occurring in what we have called above triple junctions (TJs), i.e., metal – dielectric – vacuum contacts. Under certain conditions such a contact also gives rise to EEE as a result of a microprotrusion being heated by the plasma current of an incomplete creeping discharge. Of particular interest, however, are metal – dielectric cathodes that employ ferroelectrics. In these, processes occurring in triple junctions are radically different because of the large value of ε.

3.2 Plasma formation at ferroelectric-surface triple junctions

The role TJs play in the emission of electrons from ferroelectric cathodes was studied in a series of papers [5, 27, 31 – 35] by looking at discharge phenomena at the surface of a dielectric and examining electron emission from an individual cathode – ferroelectric contact (which we will call a point cathode, or PC for short). The common arrangement used was to place in a vacuum chamber a dielectric ($BaTiO_3$) disk *1* (Fig. 4), whose one side (we will call it a metal substrate) was coated with a metal layer *2*, and to the other side of which a metal needle *3* was held down. To extract electrons from PC plasma that forms in the TJ zone, extractor *4*, acting as anode with respect to needle *3*, was used. In the first experiments [31], voltage pulses of amplitude 0.6 – 4.0 kV with a rise time of ~ 1 ns were applied between electrodes *2* and *3*. Pulse durations were taken to be $t_p = 2$, 4, 8, 20, and 50 ns. In the process of an incomplete discharge over the surface of the ferroelectric, the discharge current i_f, applied voltage U_f, and electron current from the needle – dielectric contact were registered. Depending on the polarity of the pulse on substrate *2*, needle *3* acted as either anode or cathode with respect to the substrate. The glowing of the discharge plasma and its emission spectrum were recorded. High-speed oscillographs, light amplifiers, a streak camera, a photoelectric multiplier (PEM), and spectrographs were used in the experiments. To study electron emission from the metal – dielectric contact, a positive-polarity voltage pulse was applied to electrode *4*.

A brief look at the experimental results [31] on the nanosecond pulsed surface discharge and on the electron emission from TJs is in order here. A tungsten needle and a barium titanate dielectric plate 1, 2, or 3 mm thick were used in the experiments. A discharge occurs when the amplitude of the voltage pulse exceeds some threshold value. At this instant, the lines of neutral (Ba I) and singly ionized (Ba II) barium atoms are seen in the spectrum of the plasma glow. As the voltage is further increased, other elements show up in the optical spectrum — those composing the ceramics (Ti I, O I, and O II) and the tungsten cathode (W I alone) — pointing to the destruction of the dielectric and ionization of its vapor followed by microprotrusion explosions as the emerging stages of the plasma formation (Table 2).

The surface discharge current is due to the charging of the dynamic capacitance C between the plasma moving with velocity v_d and the silver layer *2*. The velocity of plasma

Table 2. Spectral line properties of cathode glow: J, relative intensity of the brightest lines, and α, emergence probability of each line in a series of 10 discharges.

Element	$t_p = 8$ ns						$t_p = 2$ ns					
	$U = 0.8$ kV		$U = 0.7$ kV		$U = 0.62$ kV		$U = 1.63$ kV		$U = 1.5$ kV		$U = 1.4$ kV	
	J	α	J	α	J	α	J	α	J	α	J	α
Ba I	31.7	0.75	14	0.75	9.8	0.56	52.6	0.57	3.7	0.5	8.4	0.5
Ba II	22.4	0.75	9.2	0.375	2	0.33	15.4	0.75	4.34	0.5	2.24	0.17
O II	4	1	1.88	0.63	—	—	10.6	0.57	6	0.57	0	0
Ti I	19.6	0.8	1.97	0.5	—	—	18.4	0.63	4.56	0.5	1.7	0.4
W I	9.6	0.8	5.5	0.8	—	—	7.3	0.25	3.5	0.3	—	—

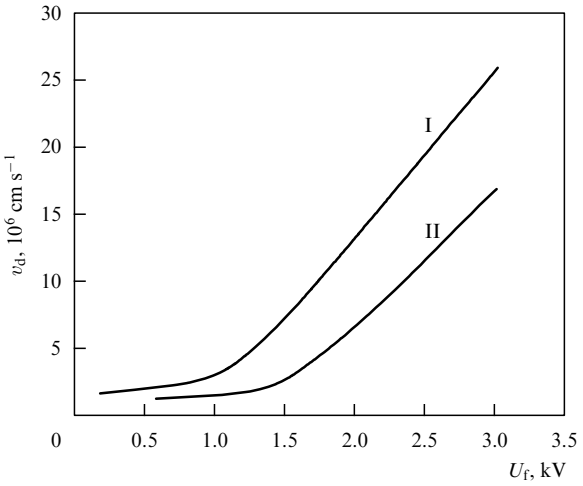

Figure 5. Velocity v_d of a discharge motion over the ferroelectric $BaTiO_3$ surface ($\delta = 2$ mm) as a function U_f of needle-to-substrate voltage; needle *3* acts as cathode (line I) or as anode (line II) with respect to substrate *2*.

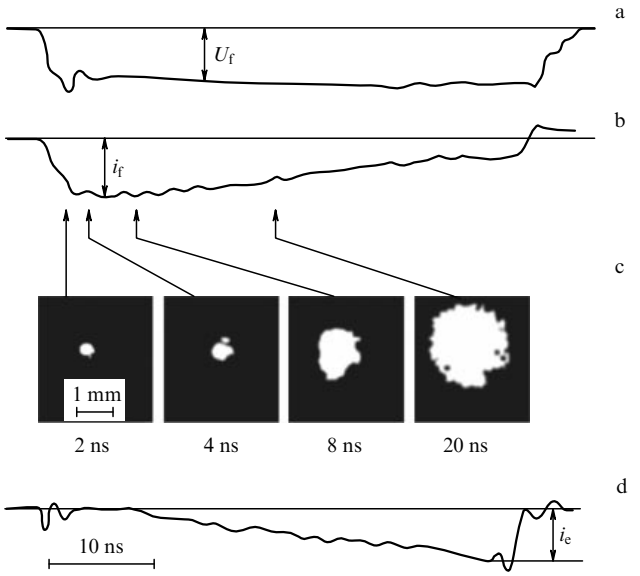

Figure 6. (a) Oscillogram of needle-to-substrate discharge voltage U_f; (b) bias current oscillogram during the development of the discharge; (c) eopogram of glow around electrode *3* – ferroelectric *1* contact at various instants of time, and (d) diode electron current versus time. Voltage pulses U_e and U_f are applied simultaneously.

motion over the ferroelectric, $v_d(U_f)$, was measured by one of the following three methods, depending on the voltage U_f applied to the ferroelectric. First, from the oscillogram of the discharge bias current i_f, because for $U_f = \text{const}$ we have $i_f = U_f \, dC/dt$. If the velocity v_d is constant, then for $v_d t < \delta$ (where δ is the dielectric's thickness) the capacitance $C = 4\varepsilon_0 \varepsilon v_d t$ and the bias current is given by

$$i_f = 4\varepsilon_0 \varepsilon v_d U_f \,, \tag{13}$$

hence, $v_d \sim i_f / U_f$, where i_f is the measured bias current, and U_f is the voltage applied between substrate *2* and tip *3*. Equation (13) is valid only for $\tau_d = 10^{-8} - 10^{-7}$ s, because for typical values of δ (1 to 3 mm) only these values of τ_d satisfy the condition $v_d t < \delta$. What makes the plasma move is the electric field tangential component at the surface of the dielectric.

Second, the velocity of the discharge motion was determined using a streak camera combined with a light amplifier [31, 34]. Figure 5 shows the function $v_d(U_f)$ for a positive and a negative tip with respect to the substrate. If the dielectric thickness $\delta > v_d t_p$, where t_p is the pulse duration, then the function $v_d(U_f)$ is at first fairly satisfactorily described by the following empirical formula [31]

$$v_d = A_0 U_f \,. \tag{14}$$

If tip *3* has a negative polarity with respect to substrate *2* (see Fig. 5), then $A_0 = 2.1 \times 10^3$ cm (V s)$^{-1}$, and for a positive polarity, $A_0 = 4.9 \times 10^2$ cm (V s)$^{-1}$. The v_d vs. U_f curve is linear only for $U_f < 1.5$ kV, after which the velocity v_d increases more than linearly with growing U_f.

And third, finally, v_d was determined from the short-circuiting of two tip electrodes in contact with the dielectric surface, for which purpose an additional tip, connected to the substrate and grounded, was placed a few millimeters from tip *3* at the surface of the dielectric. The velocity v_d determined in this way proved to be the largest of the three [34] — due in part to the fact that the presence of the second tip at the dielectric's surface strengthens the tangential electric field.

From formulas (13) and (14) it follows that the discharge current i_f for small U_f can be approximated by the expression

$$i_f = 4\varepsilon_0 \varepsilon A_0 U_f^2 \tag{15}$$

showing that the ferroelectric surface current increases in proportion to the dielectric constant ε. Experimental $i_f(U_f)$ dependences for a 2-mm-thick $BaTiO_3$ substrate for a tip having different polarities with respect to the substrate are plotted in Fig. 4. According to formula (15), the discharge current should remain constant for the length of time the pulse t_p is applied to the substrate, provided the voltage U_f is constant. As shown in Ref. [31], this occurs only during the first ~ 20 ns, and then by the instant of time $t = 50$ ns the current i_f decreases by almost half (Fig. 6).

The velocity of the plasma travel over the cathode–anode distance was estimated from the time it takes the plasma to pass the distance. For tungsten, copper, and steel tips it was found that, practically independent of the tip's polarity with respect to the substrate, the plasma velocity is $1.7-2\times10^6$ cm s^{-1} — that is, close to the plasma expansion velocity in explosive electron emission [1, 2, 26]. This finding is one piece of evidence, among others, showing that under the conditions we are considering the electron emission from a metal–dielectric–vacuum TJ is explosive due to the fact that the tips are heated by bias currents as the plasma moves over the surface of the ceramics (which occurs whether the needle is positive or negative with respect to the substrate).

In Ref. [33], the power P and the total energy W needed for a discharge were measured when investigating the energy characteristics of plasma processes on the surface of a dielectric in the presence of a point cathode. The experimental scheme used was somewhat modified from that in Fig. 4. What was new was an additional needle pressed to the dielectric plate, which was connected to the substrate and grounded. To the needle under study, a voltage pulse was applied via a cable. Steel needles 5 mm apart were used. The power P was determined as the power difference of the incident and reflected waves, which were oscillograph-recorded from the matched load of the generator, viz.

$$P = P_1 - P_2 = \frac{1}{Z}(U_1^2 - U_2^2)\,, \tag{16}$$

where Z is the wave impedance of the generator and the transmitting cable, and U_1 and U_2 are the voltages of the incident and reflected waves, respectively. The characteristics measured in paper [33] were the energy released in the surface discharge spark as a function of the voltage amplitude (which ranged from 2 to 5 kV), and the discharge power as a function of time for the interval of 5 to 30 ns. It was shown that power P is for the most part released only in the initial portion of the pulse, implying that such discharges need short-duration pulses to be ignited. Increasing the ignition pulse duration beyond 20 ns is of little or no use. The energy of the discharge amounted to 0.5–2.5 mJ.

There are four plasma sources for an incomplete discharge over a dielectric surface in a vacuum. First is the surface discharge plasma. Second, there is the plasma due to the heating, evaporation, and ionization of the dielectric's material. Third, tip *2* (see Fig. 2) explodes due to the FE current when under a negative voltage. And, finally, the fourth cause for the appearance of the plasma is the explosion of tip *1* (see Fig. 2) due to the bias current resulting from plasma motion along the surface of the dielectric.

A brief elaboration is in order here. Surface discharge plasma forms due to the presence of a tangential field component at the place where tip *1* (see Fig. 2) is in contact with the surface of the dielectric. For a needle negative with respect to the substrate, the discharge process can be pictured as follows [35–40]. Applying a voltage to the substrate results in electrons coming to the dielectric. Because the secondary emission coefficient of the dielectric exceeds unity, the place of electron bombardment will be positively charged, strengthening that field component which attracts the electrons to the insulator's surface. The atoms and ions that comprise the surface discharge plasma are those of the dielectric material and those of the gas which desorbs from the dielectric's surface during the discharge process. If tip *3* is positive with respect to substrate *2* (see Fig. 4), the surface discharge is initiated by the positive ions that the electric field causes to be emitted from the tip and which come to the dielectric's surface.

Turning now to the second plasma formation scenario, let us estimate the current density required for the evaporation of the dielectric due to the FE current from tip *2* (see Fig. 2). Suppose the dielectric surface starts to be destroyed when its temperature reaches a certain critical value $T_{\rm cr}$. Then the heating time is determined by the expression

$$t_{\rm h} = \frac{\pi\lambda\rho c}{4w^2}(T_{\rm cr} - T_0)^2\,, \tag{17}$$

where T_0 is the initial temperature, and λ, c, ρ, and w denote, respectively, heat conductivity coefficient, specific heat, barium titanate density, and the density of the energy flux impinging on the dielectric's surface. Experimentally (see Ref. [31]), it was found that $t_{\rm h}\sim10^{-9}$ s for a voltage $U\approx1$ kV. Assuming that $(T_{\rm cr}-T_0)c = W_{\rm s}$ is the sublimation heat, and that $w = jU$, where j is the electron current density, one obtains

$$j = \left(\frac{\pi\lambda\rho W_{\rm s}^2}{4t_{\rm h}U^2c}\right)^{1/2}, \tag{18}$$

which, using the specific material properties of $BaTiO_3$ [36], yields $j\approx10^4$ A cm^{-2}. Arguably, the FE current density should be about the same, because the microgap height Δ is normally very small ($<10^{-4}$ cm), so that the electric field strength at the surface of tip *2* (see Fig. 2) will be $\sim3\times10^7$ V cm^{-1} [28]. Such a field corresponds to a gap height of $\Delta\approx3\times10^{-5}$ cm in the dielectric–metal contact. This current density is 4 to 5 orders of magnitude smaller than that leading to the rapid development of an EEE current.

The third plasma formation mechanism stems from the explosion of tip *2* due to the presence of FE current in a microgap of width Δ — explaining why the spectral lines of the dielectric material precede those of tungsten in the study of Ref. [31]. The physics of this process is described in detail elsewhere [26, 41]. Section 3.3, which follows, discusses the fourth plasma formation mechanism, namely, through the emergence of EEE due to the bias-current-driven explosion of tip *1* (see Fig. 2). This mechanism is in close conformity to the law of increase of electron current in a PC diode.

3.3 Electron current in a point-cathode diode

Let us consider in somewhat more detail the role of the bias current in the emergence of EEE and in the formation of cathode plasma. At the place of contact between ceramic and an electrode there are TJs of the first and second types. Independent of the polarity of the TJ microprotrusion, a discharge similar to that shown in Fig. 6 starts at the surface of the dielectric, and the microprotrusion will short-circuit the bias current which is determined by expression (15). The bias current will flow through the metal–dielectric contact across the area $S_0 = \pi r_0^2$ (see Fig. 2), so that the current density through the contact is equal to $j = 4\varepsilon_0\varepsilon A U_{\rm f}^2/(\pi r_0^2)$, where r_0 is the radius of the microprotrusion at the TJ (it being assumed that the microprotrusion is cylindrical in shape). The metal contact will, according to formula (10), explode in a time of $t_{\rm d} = \bar{h}/j^2$, where $\bar{h}$ is the specific action which in the first approximation can be regarded as a characteristic of the

metal [27]. The explosion delay time is given by

$$t_{\rm d} = \frac{\bar{h}\pi^2 r_0^4}{16\varepsilon_0^2\varepsilon^2 A_0^2 U_{\rm f}^4} \,. \tag{19}$$

Thus, the explosion delay time of a microprotrusion is inversely proportional to the square of the dielectric constant and to the fourth power of the needle-to-substrate voltage $U_{\rm f}$. From formula (19) we obtain the inequality

$$r_0 < \left(\frac{16\varepsilon_0^2\varepsilon^2 A_0^2 t_{\rm d} U_{\rm f}^4}{\pi^2\bar{h}}\right)^{1/4} \tag{20}$$

for the tip radius r_0, below which a tip at a triple junction undergoes an explosion. For most metals $\bar{h} \approx 10^9$ A^2 cm^{-4} [27]. If $t_{\rm d} = 10^{-9}$ s, $\varepsilon \approx 10^3$, $U_0 = 10^3$ V, and $A_0 = 2 \times 10^3$ cm s^{-1} V^{-1}, then Eqn (20) yields $r < 10^{-5}$ cm. This means that within 10^{-9} s metal microexplosions will occur at all triple junctions with a contact radius smaller than 10^{-5} cm, with electrons being emitted from the metal microexplosion region due to explosive electron emission.

As shown in Section 3.1, for the vacuum diode comprising a point cathode and flat anode the EEE current in given by formula (14). For a tip placed on the dielectric substrate, the electron current $i_{\rm e}$ from the dielectric's surface can be expressed as

$$i_{\rm e} = A U_{\rm e}^{3/2} \frac{v_{\rm d} t}{d - vt} \,, \tag{21}$$

where $A = 33 \times 10^6$ A V$^{-3/2}$, $v_{\rm d}$ is the velocity of plasma motion over the dielectric, v is the velocity of plasma motion from the cathode to the anode, and $U_{\rm e}$ is the voltage that accelerates the electrons. The value of v of order 10^6 cm s^{-1} is presumably due to a microexplosion at a type 1 triple junction. From formulas (11) and (12), the ratio of the diode electron current in the presence of a dielectric to that in its absence is given by

$$\frac{i_{\rm d}}{i_{\rm e}} \approx \frac{v_{\rm d}}{v} \,, \tag{22}$$

if the cathode–anode spacing $d \gg vt$. Since $v \sim 10^6$ cm s^{-1}, and because $v_{\rm d} \sim 10^7$ cm s^{-1} for $U_{\rm f} > 2$ kV, it follows that $i_{\rm d}/i_{\rm e} \gg 1$. According to formula (21), $i_{\rm e}(t)$ is a linear function for $d \gg vt$. Although the electron current oscillogram of Ref. [31] largely supports this conclusion, it shows a current spike in its initial portion.

A study of this spike was conducted in Ref. [32] for $BaTiO_3$ ceramics of thickness $\delta = 3$ mm. Figure 7 shows electron current oscillograms for the cases in which the discharge pulse and the extraction pulse come together (Fig. 7a), the discharge pulse lags behinds (Fig. 7b), and the discharge pulse $U_{\rm f}$ leads the extraction pulse $U_{\rm e}$ by 45 ns (Fig. 7c). Over the entire range of voltages, characteristic current spikes followed by a drop-off were observed. A possible explanation of the current spikes would be an increase in the plasma potential due to the thermal electron current becoming smaller than the current extracted to the Faraday cup. Then, increasing the electron current density results in an earlier occurrence of an emission current spike, whereas increasing the plasma concentration leads to its delay. The experiments of Ref. [32] offer qualitative support for these conclusions. The dependence of the electron current on the anode-to-cathode voltage (for a positive tip-to-substrate polarity) is plotted in Fig. 8. In Ref. [31], it is shown that electron emission starts within 1 ns of the appearance of a glow on the surface of the ferroelectric.

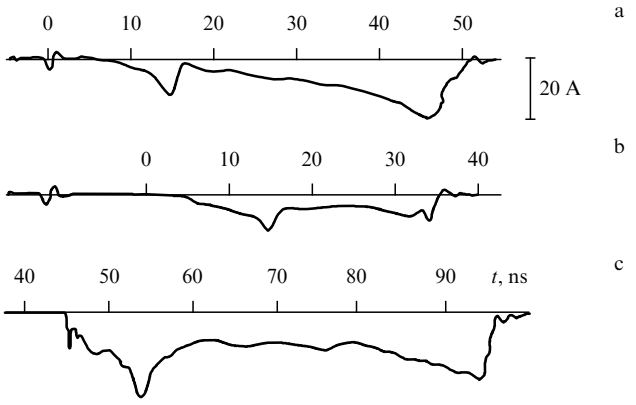

Figure 7. Diode electron current oscillograms for a point cathode on a $BaTiO_3$ surface ($\delta = 3$ mm) at a diode voltage $U_{\rm e} = 20$ kV, $U_{\rm f} = 1.2$ kV: (a) triggering voltage pulse $U_{\rm f}$ arrives simultaneously with the accelerating pulse $U_{\rm e}$; (b) $U_{\rm e}$ leads $U_{\rm f}$, and (c) $U_{\rm f}$ arrives 45 ns before $U_{\rm e}$.

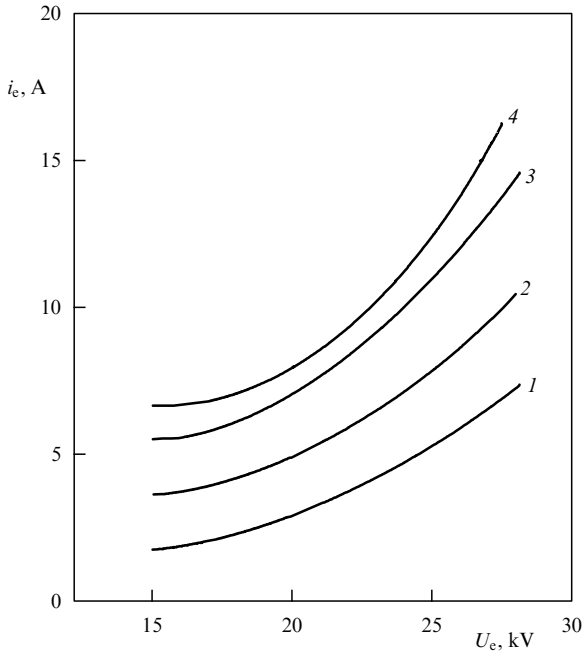

Figure 8. Electron current amplitude versus voltage applied to anode-extractor *4* for various voltage pulses and for a positive needle-to-substrate polarity: *1*, 1.8 kV; *2*, 2.3 kV; *3*, 2.75 kV; *4*, 3.1 kV.

Covering as they do a broad range of voltages and the time interval of $10^{-9}-10^{-7}$ s [31–35], the above results on the behavior of point cathodes in strong electric fields lead one to conclude that diodes with such cathodes display all the basic features of EEE:

— during the action of the pulse the diode current increases as a 3/2 power law, taking into account the cathode flare plasma expansion both in the vacuum gap and over the surface of the dielectric (if the triggering pulse does not arrive earlier than the one accelerating the electrons);

— the electron emission current, similar to EEE, exhibits instabilities in the form of short-duration spikes whose amplitude noticeably exceeds the volume-charge-imposed limitation level;

— when the pulse U_f leads the pulse U_e (the prepulse case), the diode electron current sharply increases, similar to the EEE case [26] we discussed in Section 3.1 (see Fig. 3).

4. Planar ferroelectric plasma cathodes

4.1 Background

As already mentioned, electron emission from an incomplete discharge over the surface of ceramic in a vacuum was discovered in Ref. [2]. In 1967, the authors of Ref. [4] proposed using this effect to create a high-efficiency cathode with extracting electrons from a large surface of a barium titanate ferroelectric. To create a large number of TJs, they held down a ring-shaped electrode to one side of the round ferroelectric plate and invoked silver fusing to deposit a continuous electrode on the other.

It was found, however, that in the source with a ring-shaped electrode the plasma distribution over the surface of the dielectric plate was not uniform, thus leading to a nonuniform electron beam, as will be discussed in Section 4.2. This suggested to the authors of Ref. [5] the idea of a metallic grid being placed in the inner space of — and connected to — the ring electrode. The same paper contains the first description of how an electron source with such a cathode and $BaTiO_3$ ferroelectric works. With an accelerating voltage of 50 kV, a ferroelectric cylinder thickness of 3 mm, and a pulse with an amplitude of 3 kV applied to the substrate, a 2 kA/200 ns electron current pulse was obtained. The turn-on device for the electron source used in Ref. [5] is shown schematically in Fig. 9. This device contains two pulsed electric circuits A and B, the former of which is needed for obtaining plasma on the surface of the dielectric (ferroelectric) plate, and the latter for extracting and subsequently accelerating electrons from plasma.

The cathode design exhibited in Fig. 9 has become a canonical standard for ferroelectric-based cathodes, its practical implementations differing only in the ferroelectric used and in how the front electrode grid is configured and deposited. The ferroelectrics utilized were ceramics $BaTiO_3$, PLZT, PZT, etc., whose dielectric constant varies in the range $(1-4) \times 10^3$. The solid electrode, usually called a substrate or a trigger or back electrode, was deposited on the back side of a disk-shaped ceramic sample, and the patterned electrode, called a front electrode or a grid (an actual differently shaped grid, or a strip, or ring), was applied over the emitting surface. In the first study [5], thin copper wires (30 μm in diameter) were stretched over the barium titanate surface. The patterned electrode used in Refs [9, 42, 43] consisted of 200-μm-wide connected metal strips separated by equal-width uncoated gaps, a configuration which became the 'standard' for subsequent studies. Some researchers [20, 44–46] employed a metal grid mechanically impressed onto the front (emitting) surface of the sample. Reference [35] examined ceramic samples with a grid-pattern electrode in the form of square cells made of tungsten wires 0.025 mm in diameter, their centers 0.75 mm apart. In Refs [22, 46–48], grids of standard configuration were utilized. In some experiments [15, 49], silver dye was used to glue the grid to the surface of the dielectric. One proposal [50] was a front electrode consisting of unconnected spots within the ring. In other approaches, Cu, W, Au, Ag, Pt, or Al electrodes were deposited onto the dielectric surface by tightly holding down wires [51] or using techniques such as evaporation [42, 43], ion-beam sputtering [52], photochemical etching [53], and printing [47]. A detailed study of the electrode issue was carried out in Ref. [54] employing aluminum electrodes 1 to 2 μm thick sputtered on a preliminary deposited chromium layer.

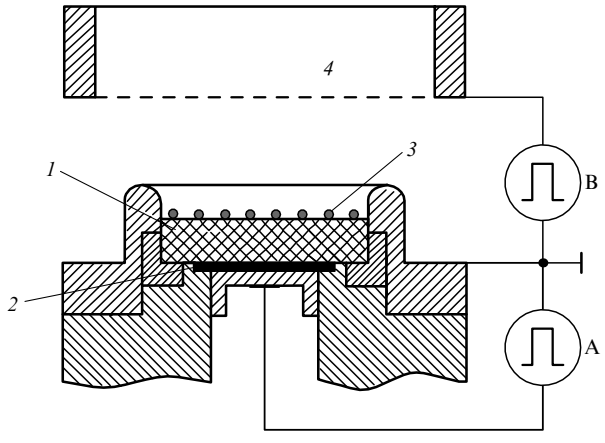

Figure 9. Schematic of a diode with a planar FEP cathode: A, electric ignition circuit for a discharge over the ferroelectric; B, electric circuit for accelerating electrons; *1*, dielectric; *2*, substrate; *3*, grid, and *4*, anode.

Whatever the grid fabrication method, however, it should be noted that the metal edges of the grid always have microprotrusions which create triple junctions independent of whether they do or do not touch the dielectric. The more such microprotrusions, the higher the degree to which the plasma fills the dielectric surface between the emitting patterns. In fact, the TJ effect will occur even when there is a microgap — rather than direct contact — between a microprotrusion and the dielectric: in this case, electric breakdown occurs between the microprotrusion and the dielectric, followed by the emergence of surface discharge of the kind we discussed in Section 3.

4.2 Physical processes on the cathode surface

We consider first what is going on at the surface of a cathode in the absence of an accelerating voltage and when a trigger voltage is applied between the front and the back electrodes. This situation exhibits optical radiation, a flux of neutral atoms and molecules, and a plasma flux. Let us consider each of these separately.

Visible radiation from the surface of a barium titanate cathode was first studied in Ref. [55], where a metal ring or thin copper wires were used as a grid. The dielectric, 4 cm in diameter, was 3 mm thick. The discharge picture for a ring-shaped grid is typically as shown in Fig. 10a, where one can see separate channels of an incomplete discharge that move from the ring towards the center of the dielectric. The duration of a pulse 5 kV in amplitude applied between ring *4* and substrate *2* was $\sim$ 100 ns. When copper wires (30 μm in diameter) are stretched within the ring, a much different picture of the discharge process emerges (Fig. 10b), involving a large number of incompleted discharges that start at the place where the wires touch the dielectric plate. In later studies [6, 49] a similar surface discharge structure for a metal-strip grid was observed in PZT samples (polar and nonpolar alike) and $BaTiO_3$ samples. Visible radiation appeared only when the electric field applied to the dielectric exceeded a certain level. Individual surface discharges usually start within the

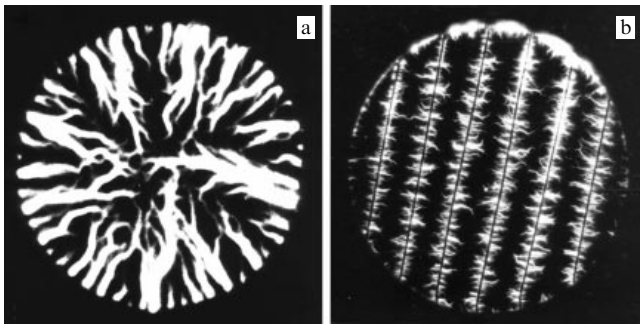

Figure 10. Glow on the surface of a ferroelectric for ring-shaped (a) and multiwire (b) grids. Integrated photos for a substrate exposed to a pulse of duration $t_p = 100$ ns, for $U_f = 5$ kV, and $d = 3$ mm.

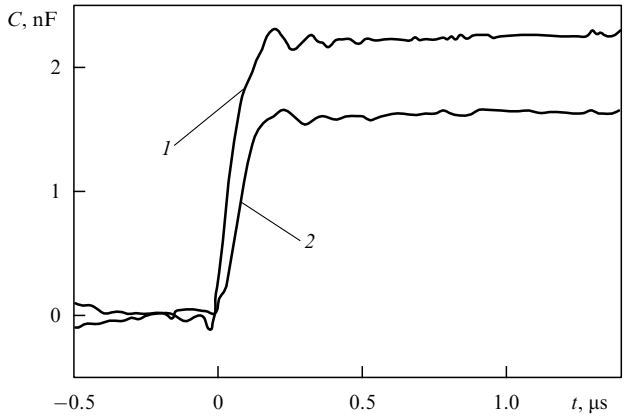

Figure 11. Capacitance between substrate *2* and grid *3* with a plasma-coated ferroelectric surface. Line *1* was obtained at positive grid voltage, and line *2* at negative grid voltage.

first few nanoseconds after a voltage pulse is applied between the front and the back electrodes. After this, the discharges start moving toward each other, and in 30 to 40 ns the whole of the surface between the strips — except a narrow region (< 1 mm) halfway in between — becomes covered by the plasma. This is typical of an incomplete discharge in which the discharge current shorts to the bias current through the dielectric, with the result that the plasma potential equals that of the grounded front electrode. Because the front edge of the surface discharge consists of an electron flux, the Coulomb repulsion between the electrons makes the discharge stop at a certain distance. Notice also that the two plasma fluxes have the same potential, which sharply weakens the tangential electric field.

The plasma moving across the dielectric surface alters the capacitance of the ferroelectric sample. Figure 11 (taken from Ref. [49]) shows $C(t)$, the variation of the capacitance with the time for a $BaTiO_3$ sample over the time period when plasma forms on its surface, for negative and positive triggering pulses 5 kV in amplitude on the grid. The curve $C(t)$ flattens to a virtually constant value in approximately 200 ns, corresponding to the time needed for the visible radiation to reach its maximum intensity. Taking into account that the capacitance of the sample with no plasma formed is ~ 1.5 nF, one can estimate the degree to which plasma covers the surface for a positive and a negative pulse on the grid. In the former case, the degree of coating is found to be much higher than in the latter.

From Fig. 11 we can obtain an approximate estimate for the average velocity of plasma motion between the strips of the front electrode. Let the dielectric be a square with a side of length $K \approx 4$ cm equal to the diameter of the circle used in Ref. [49]. Assuming in addition that the space between the strips is fully covered by the plasma, we have the following dependence for the capacitance:

$$C(t) = \frac{\varepsilon_0 \varepsilon K(a + 2v_d t)n}{\delta}\,, \tag{23}$$

where v_d is the velocity of plasma motion over the dielectric, n is the number of metal strips on the ferroelectric, a is the width of a strip, and δ is the thickness of the dielectric. Then, we find that

$$\frac{dC(t)}{dt} = \frac{2\varepsilon_0 \varepsilon K v_d n}{\delta} \approx \frac{C_\infty}{T} = \frac{\varepsilon \varepsilon_0 K^2}{T\delta}\,, \tag{24}$$

where

$$C_\infty = \frac{\varepsilon_0 \varepsilon K^2}{\delta} \tag{25}$$

is the maximum capacitance, and T is the time it takes to reach it. From formulas (24) and (25), it follows that the velocity of plasma motion over the surface of the dielectric is given by

$$v_d = \frac{K}{2nT}\,. \tag{26}$$

Because in Ref. [49] $n \approx 15$, $T \approx 2 \times 10^{-7}$ s, and $K \approx 4$ cm, it follows from Fig. 11 and relationship (26) that $v_d < 10^6$ cm s^{-1} both for a positive and for a negative grid. Hence, the velocity v_d is much smaller than that of plasma motion over the dielectric in the case of point electrodes (see Fig. 5), the reason being that the plasma motion is slowed down due to the two counter flows discussed above.

Radiation spectrum studies using the Jobin-Yvon 750 M spectrometer were performed for the ceramic that was a solid solution of $Pb_{0.7}Ba_{0.3}Nb_2O_6$, $Sr_{0.5}Ba_{0.5}Nb_2O_6$, $Sr_2Ba_4Ti_2Nb_8O_{30}$, and $BaPb_{0.33}Nb_{0.67}O_3$. According to the authors of Ref. [49], such a ferroelectric has a significantly longer service life compared to PZT and PLZT. The dielectric had an active part 70 mm in diameter and was 8 mm thick. The front and back electrodes were a copper grid and a silver film, respectively. The plasma emission spectrum revealed the presence of excited ions and neutral atoms of Cu, Pb, Sr, Ba, Ti, and O, which appeared within 50 ns after a triggering pulse with an amplitude of 8 – 10 kV was applied. The larger was the triggering pulse amplitude, the more numerous and brighter were the incomplete discharges. Thus, qualitatively, the planar cathode results of Ref. [49] were the same as the point cathode results in Ref. [31]. In both cases, the spectral lines of the cathode metal and those of the excited ions and neutral particles of the elements comprising the ferroelectric were present.

A discharge over the surface of a dielectric in vacuum is usually accompanied by an intense flux of neutral particles, due primarily to the desorption of the surface atoms and molecules [37]. In Ref. [49], Penning probes were employed to measure the parameters of such a flux for a discharge over $BaTiO_3$ and PZT surfaces. It was found that increasing the amplitude of the triggering pulse from 4 to 6 kV enhanced the Penning signal by almost a factor of three, indicating that the higher is the triggering pulsed voltage, the more intense is the neutral particle formation process. No principle difference in

the formation of neutral particles was seen between the $BaTiO_3$ and PZT samples. For $BaTiO_3$, gas pressure at the locations of the probes built up from 1×10^{-5} to 2×10^{-5} Torr within 20 μs after the triggering pulse was applied. The flux of neutral particles was estimated to move at $\sim 10^5$ cm s^{-1}. The density of the neutral particles within the 0.1-mm-thick layer from the front electrode was $n_n \sim 10^{15}$ cm^{-3}, corresponding to a few monolayers of gas. One can thus see that applying a triggering pulse deteriorates the vacuum in the system.

The parameters of the plasma flow moving from the grid to the anode of the diode were measured by using probes which were located at different distances from the grid, and using a set of collimating Faraday cups (CFCs). For example, in Ref. [49] two Faraday cups with collimating holes 0.5 mm in size had bias potentials of different polarities, allowing the electron and ion plasma components to be measured simultaneously. The influence of electromagnetic noise on the performance of the CFCs was checked by setting up a constant magnetic field in front of the collimating holes. The electron temperature of the plasma was estimated from the $I-V$ curves obtained with a single floating probe. A positive triggering pulse applied to the back electrode produced a short pulse (50 – 100 ns) of electrons before the ion signal, with the electron current density not exceeding 1.5 A cm^{-2}, and the electron energy not exceeding 400 eV.

The energy of the electrons was measured by the retarding potential method. For a negative trigger voltage on the substrate, electron energies were found to range over a broad spectrum extending from zero to several kiloelectronvolts [56]. According to Ref. [57], electrons are much more energetic for a positive than a negative pulse fed to the grid. In Ref. [9], electron energies of up to 60 eV were detected for negative pulses. The authors of Ref. [52] used an Auger spectrometer to measure electron energy for the case where a ferroelectric cathode 110 μm thick was excited by positive grid pulses. They reported a narrow energy distribution in the vicinity of 265 eV, which remains the same over trigger voltages of 300 to 400 V. Reference [58] reported on a detailed study of how the triggering regime affects the energy spectrum of electrons. If triggering pulses are applied to the back electrode, the energy spectrum is much broader than with a front electrode (i.e., the grid) application, the respective half-widths being $\sim$ 1100 eV and about 100 eV. Further, in the front electrode scenario the maximum of the spectral distribution shifts by about 400 eV toward higher energies. Thus, for a plasma that forms on a dielectric after application of a triggering pulse, the electron energy depends critically on the experimental conditions. For a review on the subject the reader is referred to paper [6].

The ion pulse that followed the electron one lasted for more than 2 μs both for $BaTiO_3$ and for PZT, and had a distinctive maximum followed by a long tail. Time-of-flight measurements revealed that the ion pulse has two components: a fast one with a velocity of $\sim 10^7$ cm s^{-1}, and a slow one with a velocity of $\sim 10^6$ cm s^{-1}. The ion current density is ~ 0.5 A cm^{-2}, which corresponds to a proton number density of $\sim 2 \times 10^{11}$ cm^{-3}. The ion flux with electrons on the front edge is due to the surface discharge plasma. The authors of Ref. [49] believe that the plasma forming during an incomplete surface discharge is accelerated away from the surface because of the presence of a magnetic pressure gradient due to the discharge current. Moreover, a positive triggering pulse fed to the back electrode can lead to an additional acceleration of ions away from the surface of the sample. The ion acceleration will cease when the negative charge of the plasma electrons kept on the front surface by the positive trigger voltage becomes equal to the positive charge of the back electrode. Reference [56] reveals a large difference between ion signals obtained with the positive and negative triggering pulses: the ion flux densities are ~ 0.2 A cm^{-2} and ~ 0.02 A cm^{-2} in the former and latter cases, respectively. This difference is likely due to the ions on the sample surface being trapped by the negative triggering pulse. In Ref. [49], it is revealed that the fast plasma flux contains ions with a velocity exceeding 10^8 cm s^{-1} at a plasma density of $10^9 - 10^{10}$ cm^{-3}. There is still no convincing explanation for this effect.

Let us consider a slow plasma flux ($\sim 10^6$ cm s^{-1}) with a density of $\sim 5 \times 10^{12}$ cm^{-3}. In our opinion, there are two reasons for this flux. First, plasma with this velocity forms when microuniformities in a metal – dielectric – vacuum TJ explode as a result of appearing a bias current due to the motion of the plasma over the surface of the dielectric. It is precisely such velocities that were measured in point cathode experiments of Refs [31, 33, 34] for both the positive and negative grid voltages (see also Section 3.2). Second, plasma with this velocity forms as a result of an explosion of the dielectric surface, which is bombarded by an FE electron beam from grid microprotrusions, provided the voltage applied to the grid is negative with respect to the substrate.

Importantly, some applications of ferroelectric plasma cathodes are unsuitable for a diode operating in the plasma-prefilled regime. Indeed, because the plasma has a high conductivity at the beginning of pulse action accelerating the electrons, the diode's regime of operation may be similar to that of a short-circuited diode. From this regime, the diode can pass to that of a plasma opening switch [1], in which its impedance increases, followed by an increase in the diode voltage and decrease in diode current. A consequence of this regime is that the energy spectrum of the accelerated electrons broadens. One way to prevent the cathode – anode gap from being prefilled with plasma is to introduce an additional control grid between the front surface of the cathode and the diode's anode. Applying a necessary bias potential to this grid can significantly decrease the flux density of fast plasma. For example, in Ref. [49] it took a control grid potential of 1.9 kV to suppress a plasma flux with a velocity of $\sim 10^8$ cm s^{-1}. Plasma fluxes at $\sim 10^7$ cm s^{-1} were suppressed by a voltage of $U_f \approx 0.7$ kV. It was found that the suppression of a plasma flux with a velocity of $\sim 10^8$ cm s^{-1} depends on the magnitude of the trigger voltage U_f: the higher is U_f, the higher is the bias potential needed for suppression.

4.3 Operation of an electron diode with a ferroelectric plasma cathode

In this section we shall show how the plasma formation method and the way in which the triggering pulse is applied to the back electrode of the cathode affect the properties of the electron beam that forms in the diode. Even early experiments with ferroelectric plasma cathodes revealed two important properties of such diodes [5]. First, the electron current in such a diode is much larger in amplitude than the Child – Langmuir current for a usual planar diode (Fig. 12). Second, the amplitude of the electron beam current depends on the delay time τ_d between the triggering pulse and the accelerating pulse. For example, at $\tau_d \approx 400$ ns this amplitude is 5 to 6 times that at $\tau_d = 0$. In Ref. [5], the sharp increase in

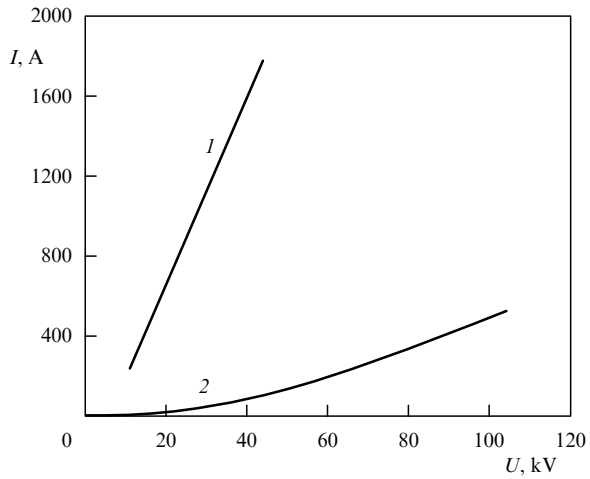

Figure 12. $I-V$ curves of an FEP-cathode diode (*1*) compared to those of a diode with a thermionic cathode (*2*).

the electron current for a large time τ_d is explained by the expansion of the plasma that forms during the pause between pulses. On the one hand, this enlarges the emitting surface but, on the other hand, it results in the negative space charge of the electrons being compensated for by ions. The maximum electron current density at the anode of a diode with an accelerating voltage of 50 kV amounted to 1.5×10^2 A cm^{-2} for a $BaTiO_3$ cathode 4 cm in diameter [5].

It is worthy of note that applying an accelerating voltage between the cathode and the anode alters the processes occurring in the cathode–plasma contact. For example, there occurs a large increase in the density of the ion current to the cathode. The interaction of this current with microprotrusions on the metal portion of the cathode and with dielectric-contaminated regions will lead to the formation of centers for the explosive emission of electrons, as occurs in a vacuum discharge [27].

On the other hand, there are two operation regimes possibly realizable in a diode with an FEP cathode: one with and the other without plasma prefilling of the cathode–anode gap. The former regime [59] features the rapid formation of a double layer near the cathode, across which most of the anode–cathode potential drops. The time needed for this is $t \approx w_e^{-1}$, with w_e being the electron plasma frequency. The initial width of such a bilayer can be estimated from the relationship

$$\Delta_p = 750\left(\frac{T_e}{n_e}\right)^{1/2}, \qquad (27)$$

where T_e [eV] and n_e [cm^{-3}] are the plasma's electron temperature and number density, respectively. From formula (27) it follows that for $n_e \approx 10^{11}$ cm^{-3} and $T_e \approx 4$ eV the width of the double layer does not exceed 5×10^{-3} cm. With a double layer that narrow, there arises a strong electric field $E \sim 10^7 - 10^8$ V cm^{-1}, which causes the explosive emission of electrons due to the large FE current from cathode microprotrusions.

The way the diode operates and the characteristics of the electron beam produced crucially depend on the parameters of the triggering and accelerating pulses. The experiments of Ref. [59] involved generators of two types with respective amplitudes of 40 kV and 250 kV. The triggering pulse was applied to the back electrode of the ferroelectric. Two depolarized ferroelectrics, $BaTiO_3$ and PZT, were used with positive or negative triggering pulses. The experiments began by observing a visible glow at the cathode and the anode. A negative triggering pulse of amplitude 3 kV and duration 10 μs was fed to the back electrode of the sample. The frame exposure time of high-speed shooting amounted to 200 ns at $\tau_d = 200$ ns. At an accelerating voltage of 35 keV, an electron beam with $t_e = 500$ ns, $j_e = 10$ A cm^{-2}, and $I_e = 80$ A was observed. After the triggering pulse reached a certain limit, the electron current was induced practically simultaneously with the application of an accelerating pulse. The same effect was observed for a point cathode (see Fig. 6). Prior to the application of an accelerating pulse, no emission was observed in the gap. On application of the accelerating pulse, light first appeared on the surface of the anode, and later a faint glow emerged on the cathode grid. 200 ns later, the emitting areas at the cathode and the anode were a few millimeters wide, with their boundaries blurred. The intensity of light in these regions dropped off almost at the instant the electron beam current ceased. The low intensity of the radiation and its steep drop testify that no explosive emission plasma is present. The observed radiation is apparently related to the plasma that results from the interaction of the electron beam with the neutral particles on the surface of the cathode. Consequently, the source of electrons operated in the plasma cathode regime [60, 61] in which the electron emission from a metal surface occurs due to ion bombardment.

The picture of visible light emission was different when accelerating voltage pulses were applied with a delay time of $\tau_d = 1.5$ μs. In this regime, electron emission began simultaneously with the application of an accelerating pulse and with an increase in electron current in the diode. A feature of the regime was the appearance of a bright layer of plasma near the cathode, which then expanded at a rate of $(1-2) \times 10^6$ cm s^{-1} and reached the anode plasma. At this instant, a jump in diode current was observed, accompanied by a sharp drop in the accelerating voltage. The reason for this is that the diode operates in the plasma-prefilled regime characterized by the formation and expansion of EEE plasma. Thus, depending on the value of τ_d, different operation regimes, with and without formation of EEE, can be achieved in the diode. The electron beam was observed to be generated at either polarity of a triggering pulse. For a positive grid voltage, however, the amplitude of the electron beam current at the same values of d, U_f, and τ_d is, all other things being equal, 2 to 3 times larger than for a negative voltage, but in either case the current exceeded the Child–Langmuir value. For example, for $U_e = 40$ kV, $\tau_d = 1.5$ μs, and $d = 2$ cm, the diode electron current amounted to 300 A, whereas the space charge-limited current should not exceed 10 A. There are two cases in which this situation can occur: either when the diode is prefilled with plasma or when some electrons leave the cathode with nonzero initial velocities. Clearly, as discussed in Section 4.2, it is plasma prefilling of a diode which plays the dominant role.

One finding of the study was that the amplitude of the electron beam current depends on the voltage U_f of the triggering pulse. Thus, increasing the voltage amplitude U_e by a factor of 1.75 increases the current amplitude by almost a factor of 6. Such strong dependence results from an increase in the density of the plasma that forms on the surface of the ferroelectric $BaTiO_3$ sample due to the large number of TJs involved.

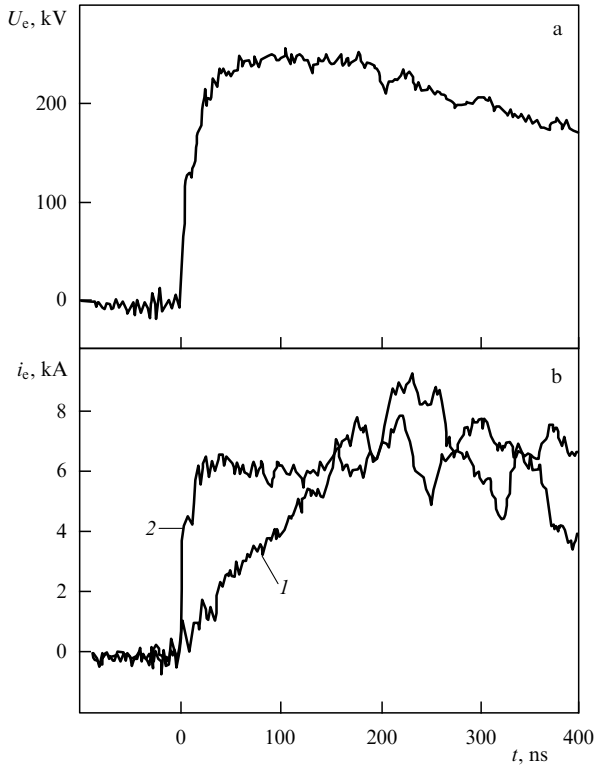

Figure 13. A typical shape of the diode voltage pulse U_e (a) and diode current i_e (b) without (*1*) and with (*2*) a plasma source in the diode. A negative triggering pulse $U_f = 6$ kV of duration $t_p = 500$ ns was applied to the substrate.

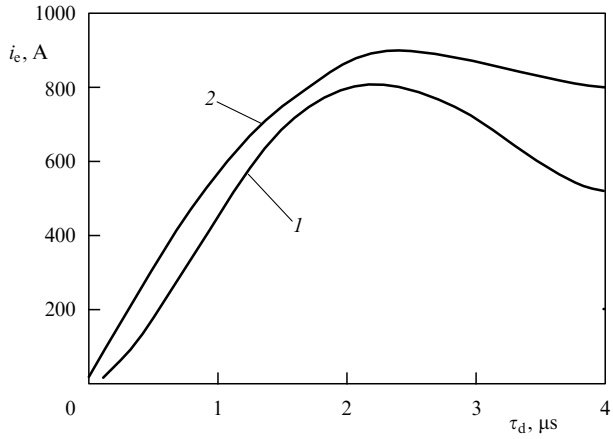

Figure 14. Diode current versus delay time τ_d. Anode–cathode gaps of lengths $d = 55$ mm (curve *1*) and $d = 45$ mm (curve *2*) were studied. Marx generator voltage was $U_a = 270$ kV. A positive 6 kV, 500 ns triggering pulse was applied to the back electrode.

Let us discuss briefly the operation of diodes with accelerating voltage $U_a \gg 100$ kV. The first electron accelerator with an FEP cathode, with an electron energy of 500 keV, a current of 10 kA, a pulse duration of 25 ns, and a current density of up to 10^3 A cm^{-2}, was developed by Bugaev et al. [62] as early as 1970. The cathode used was a barium titanate one with a copper grid stretched over the surface and with silver fused into the back side. The parameters listed above were obtained by optimally selecting the parameters τ_d, U_f, and the diameter of the cathode. Reference [56] examined an electron accelerator fed by a Marx generator with a voltage of up to 270 kV. It was shown that as τ_d, U_f, and U_e change, so does the diode electron current — a change which, nuances aside, occurs in a qualitatively similar manner to the case of a relatively low voltage U_e. The samples used in the experiments were depolarized $BaTiO_3$ and PZT ones. The pulse U_f was negative (2.5 kV for PZT, and 6 kV for $BaTiO_3$).

Typical shapes of the accelerating voltage and diode current with and without application of a triggering pulse are illustrated in Fig. 13. For $\tau_d \approx 1.1$ μs, plasma moving at a rate of $(1-2) \times 10^6$ cm s^{-1} has no time to reach the anode ($d = 45$ mm). It can, however, fill almost half of the cathode–anode gap. Results for $d \geqslant 3$ cm are qualitatively the same. For $d \leqslant 2.5$ cm, the gap is observed to be rapidly ($\leqslant 1.5$ μs) short-circuited — apparently due to the appearance of EEE and the propagation of explosive emission plasma.

There are three features to note in the observed shape of current pulses. The first is that electron emission appears with no delay with respect to the beginning of the accelerating voltage pulse in the case of an active plasma cathode. The absence of a time delay in spite of the wide anode–cathode gap and a relatively weak ($E = 60$ kV cm^{-1}) electric field points to the preliminarily formed plasma as a source of electrons. Second, the duration of the electron emission is the same in both cases, i.e., in the presence and in the absence of a source of active plasma. Explosive plasma can be produced due to the preliminary polarization of the plasma, caused by the emission of electrons in the direction of the anode, in which case the strong electric field can redistribute itself in the double layer close to the cathode output grid [63, 64]. This electric field can be the cause of the formation of explosive plasma. Third, finally, the diode current remains almost constant in amplitude for more than 800 ns.

Evidence of plasma prefilling of the diode is exhibited in Fig. 14 which depicts the dependence of the diode current on the time delay between the triggering pulse and the application of the high-voltage pulse. It is seen that the measured electron current has much larger amplitudes than predicted by the space charge law under the assumption of the presence of a vacuum anode–cathode gap. The observed electron current density $j_e \approx 230$ A cm^{-2} implies the presence of a plasma with number density of $n_e \approx 10^{13}$ cm^{-3}. Thus, the study of FEP cathodes [17, 56] under accelerating voltages of up to 500 kV demonstrated that electron beams of up to 10^3 A cm^{-2} current densities and lasting for several dozen to several hundred nanoseconds can be generated.

4.4 Ferroelectric effects

In Sections 4.1–4.3 we have shown that the operation of the cathodes we are considering here is fundamentally dominated by surface plasma acting as the source of electron and ion emission currents. This plasma forms at regions of metal–dielectric–vacuum triple contacts as a result of a surface discharge, explosions of microprotrusions on the metallic grid, or the surface of the cathode being bombarded by ions. The role of a ferroelectric as a special case of dielectric has to do with its large dielectric constant ε: in the vacuum metal–dielectric microgap (at the metal–dielectric–vacuum triple contact), the estimate by formula (7): $E_c = \varepsilon U/\delta$, with $\delta/\varepsilon\Delta \gg 1$ suggests a factor ε increase in the electric field strength. For example, applying a voltage of $U \sim 1$ kV to a $BaTiO_3$ ($\varepsilon \sim 1500$) sample $\delta \sim 1$ mm in thickness produces a field of $E \sim 1.5 \times 10^8$ V cm^{-1} in the vacuum gap of the triple contact point, a value which is quite sufficient to cause the

field emission of electrons from the metal to the vacuum gap. The electrons that are emitted from the metal are initial electrons for generating plasma on the surface of the dielectric (i.e., ferroelectric $BaTiO_3$ in our case).

However, along with the interpretation discussed in Sections 3.2, 3.3, and 4.1–4.3 [and based on formula (7)], there exist other interpretations in which the emission of electrons is explained by the distinctive properties of ferroelectrics. Of particular note are two of these: one completely ignoring the existence of plasma, and the other assuming that plasma can be created due to ferroelectric effects.

The interpretation which ignores the existence of surface plasma and its participation in the process of electron emission from ferroelectric cathodes [1] was applied in various versions to experiments that did not examine the presence (or absence) of surface plasma. It is in these studies [7, 15, 17, 42, 43, 45, 56, 65–70] that no check was made for the presence (or absence) of the current of the ion emission which occurs simultaneously with the electron emission. Such a check is a decisive experiment to prove (or disprove) surface plasma participation in the process of electron emission from ferroelectrics.

However, the late 1990s experiments on ferroelectric ceramics PLZT 12/65/36 [15] and PLZT 7/65/35 [71], and ferroelectric TGS [20] showed that, without exception, in all ferroelectric regimes electron emission from ferroelectrics occurs from the plasma that forms on the surface of the dielectric. The check for the simultaneous presence of the currents of emitted electrons and emitted ions [15, 20, 71] provided direct experimental verification of the emergence of surface plasma and of its critical role in the electron emission process — thus justifying the undisputed rejection of all speculative no-surface-plasma scenarios of strong electron emission from ferroelectric cathodes.

Experimental research on the ferroelectric cathodes, described in Sections 4.1–4.3, reveals the critical role of the plasma that forms on the surface of the cathode. The process of the plasma creation on the emitting surface of a ferroelectric cathode depends fundamentally on the metal–dielectric–vacuum TJ. This was shown in studies by Mesyats's team in Russia (both old [2–5, 31–34, 36, 62, 72, 73] and recent [27, 35, 41, 55, 74, 75]) and Krasik's team in Israel (see, for example, Refs [6, 15, 20, 49, 58, 59, 76]). There is, however, recent evidence that in some situations the production of plasma on the frontal (emitting) surface of a ferroelectric cathode cannot be explained in terms of a triple junction discharge. Let us briefly discuss the arguments presented in Refs [20, 71] for the matter. What we will see is that paper [20] does indeed discuss a situation where the triple junction discharge fails to explain the appearance of surface plasma, but the arguments of Ref. [71] are not convincing.

[1] In these versions, the fast (nanosecond) inversion of ferroelectric domains, the fast change of the ferroelectric's polarization state, or a fast phase transition induced by the applied field [6] was the assumed reason for the high current density of electron emission. It is believed that, as a result of the fast changing of spontaneous polarization, the strong internal field of noncompensated bound charges in the surface layer leads to the extended spontaneous emission from the ferroelectric material to the vacuum [7]. According to Ref. [56], electrons are freed from local donor levels produced due to the La doping of PLZT ceramics. It is assumed that donor centers are particularly concentrated near the surface of preliminarily polarized samples, a region from which electrons are liberated when ferroelectric domains are repolarized.

To demonstrate the role of repolarization in the creation of surface plasma and the subsequent electron emission, the authors of Ref. [20] used the 'model' (or 'classic') crystals of TGS, a material from a class of ferroelectrics that had been studied most [77, 78]. TGS (spontaneous polarization $P_s = 2.8\ \mu C\ cm^{-2}$, $\varepsilon \sim 50$) is easily repolarized in electric fields of several hundred volts per cm, thus readily allowing the study of the basic physical aspects of the phenomenon. Furthermore, because of its low Curie temperature, $T_C = 49\,^{\circ}C$, the crystal can be easily changed over to the paraelectric phase through heating.

From formula (7), inserting $\varepsilon = 50$ and $U/\delta = 500\ V\,cm^{-1}$, we find that in the microscopic vacuum gap of a dielectric–metal–vacuum TJ the electric field strength does not exceed $E = 2.5 \times 10^4\ V\ cm^{-1}$, and hence is not strong enough for initial electrons to be field-emitted either from the metal or the ferroelectric. In other words, this estimate shows that if a ferroelectric cathode is made from a TGS crystal and if the triggering pulse applied to it is of low strength (on the order of the TGS coercive field $E \sim 500\ V\ cm^{-1}$), then under such conditions triple contact points cannot play a crucial role in the process of the creation of surface plasma.

A rigorous experimental confirmation of this conclusion was obtained in Ref. [20], whose basic results can be summarized as follows.

(a) In a ferroelectric phase (for $T < T_C = 49\,^{\circ}C$), the application of bipolar repolarizing pulses with a field strength of $E \sim 500\ V\ cm^{-1}$ to the ferroelectric cathode leads to the generation of plasma on its frontal (grid-covered) surface, from which electron and ion currents with a density of several amperes per cm^2 are emitted into the vacuum. But if the TGS crystal is transformed into the paraphase by heating it to $T > T_C$, then no plasma creates on the frontal surface and no electron or ion emission is present. This proves experimentally that under the conditions described the metal–dielectric–vacuum TJs have no role in the creation of surface plasma, because the dielectric constant has the same value ($\varepsilon \sim 50$) both in the ferroelectric phase ($T < T_C$) and in the paraphase ($T > T_C$).

(b) Both in the ferroelectric phase ($T < T_C$) and in the paraphase ($T > T_C$), the application of unipolar triggering pulses with a strength ranging from $E \sim 500\ V\ cm^{-1}$ all the way to $E \sim 1.25 \times 10^4\ V\ cm^{-1}$ (where no repolarization occurs) does not produce front surface plasma, with the result that both electron and ion emission currents are absent. This further confirms that under the indicated conditions TJs are of no relevance to the creation of surface plasma.

(c) The results presented in (a) and (b) items show that under the conditions described surface plasma (if it creates at all) is not produced by processes in metal–dielectric–vacuum TJs, but rather by repolarization processes in the domain structure. Precisely how these latter lead to the generation of surface plasma is another matter. A perfect description of how the domain structure repolarization produces surface plasma is perhaps a task for the future. As of now, it is hypothesized that the weak ferroelectric emission of initial electrons (with current densities of order $10^{-7}\ A\ cm^{-2}$) may occur in the strong fields of noncompensated bound charges, followed by their avalanche multiplication in tangential electric fields between nonequilibrium 180° domains [20, 71].

We now turn to a discussion of the arguments presented in Ref. [71]. In this work, PLZT 7/65/35 ceramics were chosen

to comparatively study surface plasma electron emission in the repolarization and nonrepolarization regimes (which are sequences of bipolar and unipolar triggering pulses, respectively). On the one hand, this composite has a high dielectric constant comparable to that of the ceramic composite PLZT 12/65/35, a material in which electron emission was observed in the paraelectric phase [15, 69] (i.e., surface plasma was indisputably produced due to triple junction discharges). On the other hand, PLZT 7/65/35 is a composite with high spontaneous polarization reaching several dozen microcoulombs per cm^2, so that one and the same sample of this ferroelectric ceramics allows the comparative study of strong electron emission in the repolarization and nonrepolarization regimes. The results obtained in Ref. [71] can be summarized as follows.

(α) The ceramic PLZT 7/65/35 was investigated only in the ferroelectric phase.

(β) In the case where bipolar pulses are applied, i.e., in the repolarization regime, the trigger voltage that produces surface plasma and gives rise to the subsequent electron and ion emissions was 2 to 3 times lower than if unipolar pulses were applied (nonrepolarization regime).

(γ) In the nonrepolarization regime, electron emission can be excited both by short-duration ($\tau_p < 300$ ns) and by longer-duration voltage pulses, whereas in the repolarization regime it ceases when short ($\tau_p < 300$ ns) voltage pulses are applied.

The above results first of all led the authors of Ref. [71] to agree that in the nonrepolarization (unipolar triggering) regime surface plasma is initiated by triple junction discharges. These authors believe, however, that in the repolarization (bipolar triggering) regime a different surface plasma initiation mechanism — one involving the reversal of spontaneous polarization — is involved.

We find this interpretation less than convincing, however. Of those experimental results listed under items (α) to (γ), none is at odds with the assumption that there are three mechanisms that provide the initial electron emission necessary for the initiation of surface plasma, namely: the field emission in the strong electric field of microscopic gaps in triple junctions; explosive emission in triple junctions, or electron emission from metal due to the bombardment of the metal surface by positive ions [60, 61]. The decrease in the amplitude of triggering pulses in the repolarization regime by only 2 to 3 times may result from the fact that, compared with the nonrepolarization regime, in this regime an additional tangential electric field is induced by the nonequilibrium bound charges of 180° domains, charges that arise due to repolarization and which strengthen the tangential accelerating field and thereby facilitate the formation of plasma. The disappearance of electron emission upon applying short bipolar triggering pulses could be explained by the fact that 180° domains do not have enough time to form, and that an additional tangential accelerating field needed for surface plasma creation does not emerge.

Thus, there is no convincing case for supporting the view made in Ref. [71] that, in the repolarization regime in PLZT 7/65/35 ceramics, the plasma-initiating initial electrons arise from weak 'ferroemission' rather than from triple-point processes.

So, the bottom line of the entire body of available experimental data is that, first, electron emission from ferroelectric cathodes occurs from surface plasma, and, second, the initial electrons needed for the plasma to form are generally produced due to processes at triple junctions (where the metal, dielectric, and vacuum come together). The only exception to the latter rule is electron emission from the low-dielectric-constant ferroelectric TGS [20]. Laser-induced electron emission from a ferroelectric was observed in Ref. [76]. A detailed description of this effect is given in review [6].

5. Devices using ferroelectric plasma cathodes

5.1 Operational features of diodes

As discussed in Sections 4.1 – 4.3, FEP-cathode diodes can provide much higher electron current densities j than their thermionic counterparts. This is the great advantage of FEP cathodes. Even in the pioneering work [5], where such (barium – titanate-based) cathodes were proposed, electron current densities of $j_e = 150$ A cm^{-2}, an order of magnitude larger than the Child – Langmuir value, were reported. Later on, with the reemergence of interest in such cathodes, an electron current density of order 10^2 A cm^{-2} was obtained in Ref. [79], as well as in Refs [9, 14, 16, 44 – 46, 50, 59]. In Ref. [53], thermionic and ferroelectric cathodes were compared for one and the same gun design. The cathode-to-anode voltage in the diode was kept constant, and a triggering pulse was applied to the substrate. As was the case in Ref. [5], under the same experimental conditions an FEP cathode produced a current an order of magnitude larger than the thermionic cathode (the total current was 36 A). The brightness of the beam for a current of 15 A and a voltage of 10 kV amounted to $\sim 10^{11}$ A m^{-2} sr^{-1}. It should be noted, however, that the measured values of brightness varied from work to work. For example, in Ref. [45] the brightness was 10^9 A m^{-2} sr^{-1} for a current of 42 A and a voltage of 21 kV.

Importantly, FEP cathodes allow high electron currents to be obtained. To quote from as early a study as that of Ref. [5], "as the extracting voltage increases, the electron current increases linearly, reaching 1.8 kA at a charging voltage of 45 kV." First discovered in Ref. [5], the linear dependence of the current on the voltage was invariably observed in all works on FEP cathodes. However, the duration of this current in Ref. [5] did not exceed 100 ns. In later papers [16, 57, 80], a kiloampere current was achieved in the microsecond interval. The way an FEP cathode is put in operation influences the diode $I-V$ curve because the trigger voltage can be applied either to the substrate or to the grid. Furthermore, the triggering pulse can be either positive or negative in polarity. The emission current of FEP cathodes and the emitted electron energy as a function of the triggering regime were studied in Refs [16] and [57], respectively. Reference [58] demonstrated the key role of the triggering regime in the broadening of the electron energy spectrum and in determining the perveance of the electron beam.

The perveance P, defined by the relationship $P = i_e/U_e^{3/2}$, where i_e is the gun current, and U_e is the voltage, is one of the most important parameters of an electron gun. For a negative trigger voltage, gun perveance values of 67 μA $V^{-3/2}$ and as low as 11 μA $V^{-3/2}$ were measured, depending on whether the pulse was applied to the front or the back electrode [58]. However, both these values are an order of magnitude larger than typical for thermionic cathodes. A perveance of about 280 μA $V^{-3/2}$ was achieved with a plasma-cathode electron gun using the extraction of electrons from hollow-cathode

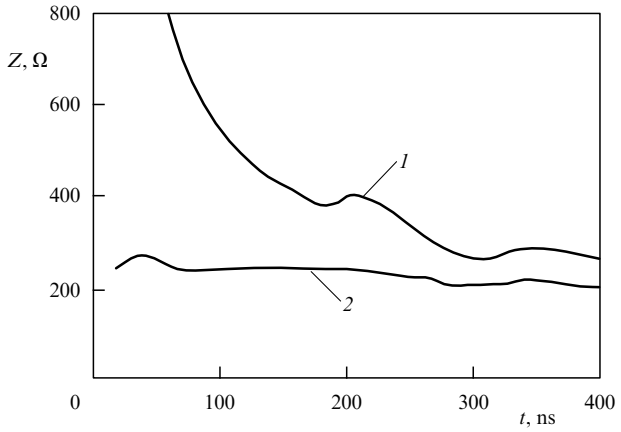

Figure 15. Time dependence of diode impedance in the absence (*1*) and in the presence (*2*) of a triggering pulse. Marx generator voltage was $U_a = 270$ kV. A $BaTiO_3$ sample was placed at 3 mm from the output cathode grid. A positive triggering pulse of 6 kV in amplitude and 500 ns in duration was applied to the back electrode. Delay time was $\tau_d = 1.1$ μs.

discharges [81]. It can be concluded that the high perveance typical of plasma cathodes can also be achieved with FEP cathodes based on the extraction of electrons from surface discharge plasma. A perveance of $10-15$ μA $V^{-3/2}$ with a back-electrode negative triggering pulse was also achieved in Refs [45, 53].

As discussed in Section 4.3, the important factor affecting the parameters of an FEP cathode is the length of time between the instants when the triggering pulse is applied to the ferroelectric sample and when the accelerating cathode–collector voltage is turned on. A number of studies [45, 57, 80] have shown that the delay in the application of voltage to the gap has an optimum value which maximizes the current density of the ferroelectric cathode. Experimentally, the optimum delay time was found to range between 0.4 and 5.0 μs. Outside this range, the current drops off or disappears completely.

The experiments of Refs [49, 59] investigated the impedance of an FEP-cathode diode. It was shown that the diode impedance strongly depends on the time delay of the application of the triggering pulse with respect to the beginning of the accelerating pulse. If plasma does not prefill the anode gap, the diode impedance decreases during the action of the accelerating pulse due to the expansion of the explosive emission plasma. In the absence of explosive emission plasma and in the presence of an unlimited source of electrons, the diode impedance Z_d should be proportional to $U_a^{-1/2}$. Experimentally, however, the impedance was found to increase or be quasiconstant, which cannot be explained unless plasma preliminarily fills the anode–cathode gap (Fig. 15). It was found that the plasma prefilling regime can produce an electron beam with the current density of several hundred amperes per cm^2 (with the application of an accelerating voltage pulse of several dozen kilovolts). With the properly selected values of τ_d, U_f, U_e, U_a, and d, an electron beam of several hundred nanoseconds in duration was observed. In addition, depending on the values of τ_d, U_f, U_e, and d, operation regimes with or without the formation of explosive emission plasma were observed. Moreover, a regime with a quasistationary plasma boundary was observed, in which the impedance of the diode is almost constant.

A few remarks are in order to conclude this section. First, various studies yielded different results concerning diode parameters. This can be explained by diverse experimental conditions. However, none of the studies has questioned the fundamental conclusions concerning the role of the parameters τ_d, U_f, U_e, and d. Second, two serious drawbacks of FEP cathodes are the emission of fast fluxes of ions and neutral particles that deteriorate the vacuum, and the wide energy spread of the electrons emitted by such cathodes. This prevents the use of FEP cathodes in a number of applications. Third, FEP cathodes have so far had a limited service life [6, 20, 47, 82] which does not exceed 10^6 pulses, with each pulse lasting several hundred nanoseconds. What prevents the operation of a cathode is the destruction of the grid metal and the mechanical destruction of the ceramics. These destructive effects arise from the physics governing the operation of the FEP cathode. The material of the grid is ablated due to the explosions of microroughnesses at the surface of the metal or because the metal is sputtered by positive ion bombardment. Other processes involved include the ion sputtering of the ceramic surface and the evaporation of the ceramics due to the energy transfer by the ions. Yet another ceramic destruction mechanism is the heating of its microregions by the field emission electrons.

All this notwithstanding, FEP cathodes offer a number of very important advantages over thermionic cathodes: an order of magnitude larger electron current; ease of operation; the capability of operating under poor vacuum conditions ($\sim 10^{-5}$ Torr), and no need for constant heating. Finally, their very low cost makes them attractive for many applications.

5.2 Application of ferroelectric plasma cathodes

The FEP-cathode accelerator developed in Ref. [62] had an electron beam energy of 500 keV, a current of 10^4 A, and a pulse duration of 25 ns, and was originally designed for research in solid-state radiation physics, in particular, to imitate ionization processes in the tracks formed by cyclotron protons in dielectrics when passing through them [83]. The accelerator's cathode, made of barium titanate, was 3 mm thick, 4 cm in diameter, and 1 cm away from the anode. The test of the cathode at a voltage of 50 kV was described earlier in Ref. [5]. The substrate of the cathode was formed by sputtering silver, and the front electrode consisted of copper wires stretched over the dielectric. The schematic of the accelerator is presented in Fig. 16. Inside metallic tube *2* are placed pulse transformer *4*, storage device *5* in the form of a coaxial line segment, chamber *6* with high-pressure spark gaps, and an accelerating tube. Energy is first accumulated in charging capacitor *1*, which is located outside of the tube and connected to the transformer's winding by a strip line. To turn capacitor *1* on to the winding, an air spark gap *3* was used. The transformer design follows the autotransformer scheme [1].

The upper part of tube *2* that houses the transformer is filled with the transformer oil. A storage coaxial line *5* with glycerine, which was selected as a dielectric because of its large dielectric constant, is placed in the lower part of the tube. Following the storage line, the peaking (*7*) and chopping (*8*) spark gaps are mounted, operating at a nitrogen pressure of 12 atm.

The accelerating tube, insulated by organic glass from a chamber with spark gaps, contains cathode *9* and a thin-Ti-foil anode *10* for extracting the electron beam. The vacuum

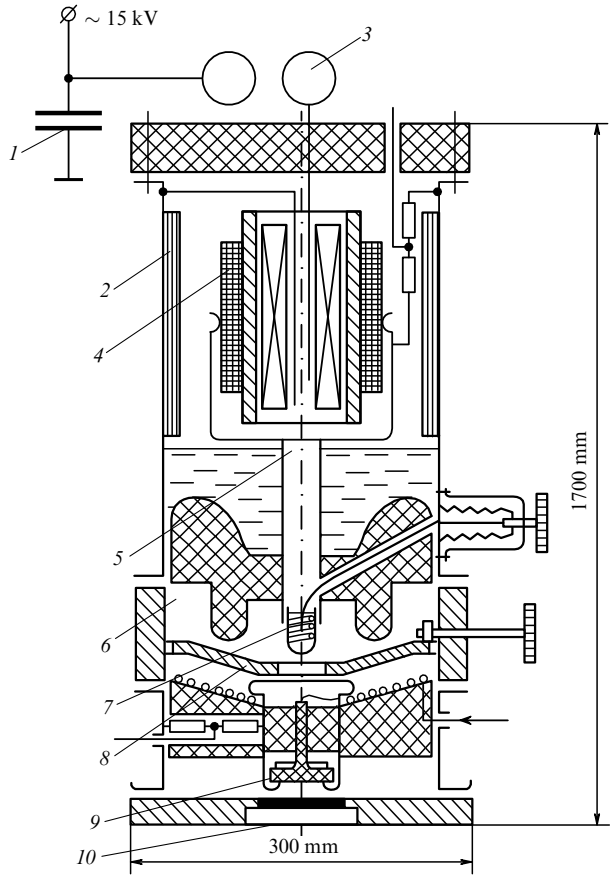

Figure 16. Schematic of an accelerator: *1*, charging capacitor; *2*, tube; *3*, spark gap; *4*, pulse transformer; *5*, storage device; *6*, spark gap's chamber; *7*, peaking spark gap; *8*, chopping spark gap; *9*, cathode, and *10*, anode.

within the accelerating tube was 10^{-5} Torr. The explosive emission cathode consisting of 1600 tungsten needles uniformly arranged at a 4-cm-diameter cathode 1 cm from the anode produced a current of about 1 kA at a cathode – anode voltage of 500 kV. To increase the amplitude of the pulse, a ferroelectric barium-titanate plasma cathode was utilized, with which an electron current of about 10 kA was obtained.

We next refer to the electrical circuit in Fig. 17 to consider the operation of the accelerator. The operation of spark gap *3* makes capacitor *1* (1 μF, 15 kV) discharge on the winding of pulsed autotransformer *4*, causing storage line *5* to charge to a voltage of 500 kV within 470 ns. This voltage is detected by ohmic voltage divider *11*. The gap of the peaking spark gap was set such that its breakdown occurred at the peak of the voltage pulse. The operation of the spark gap gives rise to a voltage pulse with a 7-ns rise time on the diode. The pulse trailing edge is formed using the chopping spark gap. The duration of the pulse can be varied by varying the length of the gap in spark gap *8*. The cathode voltage is detected by ohmic voltage divider *12*. The operation of spark gap *3* causes a voltage of 10 kV to be applied to the discharge circuit of the cathode. This pulse is sent along Archimedes-spiral cable *13* laid on the insulator and arrives earlier than the high-voltage pulse. Varying the delay time changes the amplitude of the electron current. The current of accelerated electrons was detected using Faraday cup *14* and noninductive shunt *15*. It is noteworthy that the electron current density in this accelerator reaches 10^3 A cm^{-2}, almost ten times the Child –

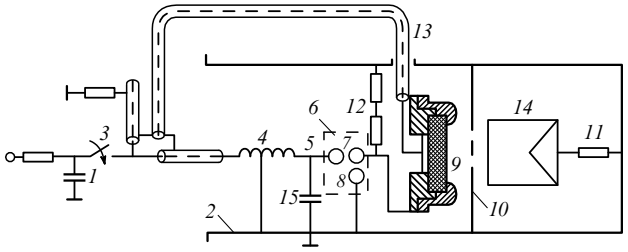

Figure 17. Electrical circuit of an accelerator: *1 – 10*, the same as in Fig. 16; *11* and *12*, voltage dividers; *13*, cathode power cable; *14*, Faraday cup, and *15*, glycerine-line capacitor.

Langmuir current density. A description of how this accelerator and its various modifications work can be found in Refs [1, 48, 51, 72].

In the electron accelerator developed in Ref. [70], a laser pulse is used to excite emission from a grid-coated ferroelectric. Although this emission was explained as resulting from Auger processes in electron layers [6], we rather believe that it is due to the plasma created by the laser beam on the surface of the grid [73].

The FEP cathode was used as a basis for developing an electron gun capable of producing a current of several hundred amperes at a voltage of 500 keV [84] and intended to produce high-power microwave radiation using a traveling wave tube (TWT) amplifier. The ferroelectric cathode 1 mm thick and 2.8 cm^2 in area was made of PZT ceramics. A thin grid consisting of a set of 200-μm-wide silver strips 200 μm apart was deposited on the front surface of the ferroelectric. The grid was grounded, and a positive triggering pulse 1 kV in voltage was applied to the back surface of a ferroelectric sample. The emission observed was 250-ns pulses with a repetition rate of 1 Hz. An electron current density of 125 A cm^{-2} was obtained. The rise time of the electron beam current was less than 20 ns.

The authors of Ref. [6] believe that high-quality pulsed electron guns utilizing FEP cathodes can be developed for use in high-power microwave generators. According to Ref. [85], high-power continuous (or long-pulse) gyroscopic devices mainly rely on thermionic cathodes. Short-pulse high-power gyroscopic devices also employ guns with an explosive emission cathode [85]. High-current FEP cathodes have a chance to change the situation in this field, as preliminary results on their use in a gyrotron microwave generator [6] suggest. For example, an FEP cathode was used in a cyclotron resonance maser (CRM) in Ref. [86]. The CRM generator operated at a frequency of ~ 7 GHz, close to the cut-off frequency of a hollow cylindrical cavity. The cathode was made from PLZT ceramics with a high dielectric constant ($\varepsilon \approx 4000$). Electrons were extracted from the plasma that was excited on the surface of the cathode by $\sim$ 1-kV, short-rise-time voltage pulses. FEP cathodes are likely to advance microwave device technologies to other applications.

The cathode constitutes a key element in microwave devices, cyclotron resonance masers, and free electron lasers, the features of the cathode and its sensitivity to operating conditions being crucial to the performance of the device. FEP cathodes have attractive features in this respect. They can be operated in a poor vacuum, at room temperature, and at low voltages comparable to those with carbon-fiber cathodes [87]. Moreover, they do not need heating or preactivation, and are easy to fabricate and use compared to

their thermionic, field, or explosive emission counterparts. There have been made proposals to use FEP cathodes as electron beam sources for free electron generators or cyclotron resonance masers [7, 9].

One of the applications of electron diodes with FEP cathodes was for triggering gas discharge spark gap switches. A low-pressure hollow cathode switch triggered by a pulsed electron beam from an FEP cathode was developed at CERN for the Large Hadron Collider [66]. The electron beam was transported from the hollow cathode region to the main gap of the switch to initiate (with nanosecond precision) a gas discharge with a current maximum of 45 kA [7]. In Ref. [88], a ferroelectric cathode was employed to trigger a radial, multichannel pseudospark switch. Distributing the current over several discharge channels allows large discharge currents to be achieved.

Electron beam modulation and the generation of high-frequency radiation in an FEP-cathode diode were observed in paper [89] using a pulsed voltage of 25–45 kV with $BaTiO_3$ and PZT cathodes. The plasma was created by applying a pulse of several kilovolts to the substrate with a delay time of ~ 500 ns. The frequency of the high-frequency radiation amounted to 320 MHz, its duration was $\geqslant 1$ μs, and it had a power of 30 kW.

5.3 Plasma cathodes versus ferroelectric plasma cathodes

Plasma electron sources are used widely in a variety of technological devices [60, 61], their plasma generation mechanisms including arc, glow, magnetron, hollow-cathode, and other types of discharges in a low-pressure gas. In this respect, plasma- and FEP-cathode diodes have much in common because in both cases it is plasma which is used as an intermediate element to extract electrons from the surface of a metal cathode. In particular, Refs [90–92] explored the possibility of using FEP cathodes in devices analogous to grid-stabilized plasma cathodes [61, 93–98]. Such systems are advantageous in utilizing electron emission from a uniform, quasistationary plasma boundary, thus allowing for current pulses with a long duration and with electrons distributed evenly over the cross section. The references above compared grid plasma cathodes (GPCs) with FEP cathodes and with low-pressure-arc GPCs with geometrically screened and unscreened cathode spots [93] as used for obtaining wide kiloampere electron beams of submicrosecond duration.

GPC studies in the 1970s–1980s by Kreindel's group in Tomsk and Zharinov's group in Moscow [60, 93–96] focused on the properties and fundamental operational aspects of GPCs, such as the role of the hollow anode, conditions for effectively extracting plasma electrons, how to enhance the emission uniformity, the key role of the grid, the pressure effect on the rate of discharge establishment, and the effect of electron extraction on the plasma potential. In Ref. [95], the theory of the GPC was developed and the role of the grid was examined. The first experiments on the employment of GPCs to obtain kiloampere microsecond beams were conducted in Ref. [97]. In Ref. [98], the hollow-cathode discharge was for the first time effectively used to obtain high-current electron beams.

Because the direct utilization of FEP cathodes in high-voltage electron sources poses some problems, due to the effect of the accelerating voltage on the emitting plasma, the authors of Ref. [99] came up with the idea that this powerful plasma source might be incorporated into a hollow-electrode grid plasma cathode. A hollow electrode makes it possible to create an electron emitter with a less dense but more uniform plasma with a large emitting surface, whereas the grid diminishes the influence of the accelerating field on plasma generation, thus stabilizing the operation of the plasma emitter.

Although originally the idea of Ref. [99] was simply to employ the FEP cathode for igniting a hollow-cathode discharge by injecting auxiliary plasma, a series of follow-up papers clearly demonstrate the authors' progress in understanding the operation of GPCs. What they realized was that the hollow cathode itself contributes little to electron emission, but that in this electrode system after-emission occurs in the FEP cathode, supported by plasma residing in the cathode cavity. This emission gives rise to a longer-duration electron emission current and makes the electron emission more uniform. An important aspect studied in Ref. [99] is how gas pressure and the size of the hollow cathode affect the magnitude of the electron current. A discharge with a current of up to 1 kA was obtained, originally lasting for 10 μs and then for several hundred microseconds. It is found [99] that 85% of the electron current is supplied by the FEP-cathode's plasma. Simultaneously, the role of the hollow cathode as an emitter was found to be small and consisted only in securing the oscillation of a part of the electrons and in making the near-grid plasma more uniform.

Because in a hollow-cathode system the discharge contribution amounts to very little and depends on the pressure, the authors of Ref. [100] turned to a hollow-anode system capable of operating at lower pressures. This suggested using higher discharge currents, so that such systems and those with an FEP cathode could be compared properly for their properties. It is found that hollow-cathode and hollow-anode systems differ in that their plasma-to-wall potentials differ by 100 V. However, both types of systems showed electron oscillations, an effect which facilitates the generation and enhances the uniformity of plasma. A major concern of Ref. [100] was the operation regimes of the GPC grid. In this context, the self-bias operation regime was proposed for the first time, which mitigates the effect of plasma prefilling the gap and helps to stabilize emission; two other initial observations were an increase in plasma potential of up to 3–6 kV during the extraction of electrons, and emission self-locking at the fall-off of the high-voltage pulse. By self-biasing the grid potential, the authors of Ref. [100] diminished the supply of plasma to the gap and were able to realize the operation of the diode in the space-charge current-limitation regime by properly selecting the delay time (12.5–15.5 μs) for the high-voltage pulse. This made it possible to eliminate the appearance of cathode spots on the grid, to make the diode highly stable in operation, and to achieve shape reproducibility for a 1-kA, 0.3-μs beam pulse at a voltage of 200 kV [101].

To summarize, depending on the conditions, FEP cathodes can operate, on the one hand, in a regime close to that of explosive emission cathodes, and, on the other hand, in the plasma cathode regime. The former, as shown in Section 3.3, certainly occurs for nanosecond electron beam pulses. The latter apparently occurs for microsecond pulses. It is a moot question, however, exactly how electrons are extracted from the cathode in the plasma regime. It is not unlikely that the EEE and plasma regimes exist simultaneously in the microsecond range.

6. Conclusions

In his 1966 experiment on a pulsed discharge over the surface of ceramics in a vacuum, the present author observed [2] cathode electrons being emitted from a metal – dielectric – vacuum triple junction under the conditions of an incomplete discharge. Central to this process is the presence of the large electric field tangential component at the surface of the dielectric. Even back then, the effect found applications in metal – dielectric cathodes, whose special feature was a large number of TJs. A radical increase in the efficiency of such cathodes was achieved by the use of a ferroelectric ($BaTiO_3$). On the emitting side was placed a metal grid held down to a ferroelectric plate, whereas the other side of the ferroelectric was sputter-coated with a layer of metal. This layer was termed a substrate. If the grid is grounded and the substrate is subjected to a voltage pulse, then a large number of incomplete electric discharges originating from the triple junctions appear on the surface of the dielectric. Placing the anode at a certain distance from the grid in a vacuum and subjecting it to a positive accelerating voltage produces in such a diode an intense flow of electrons from the cathode.

An accelerating voltage of 50 kV produced an electron current density of 10^2 A cm^{-2} at a total electron current of around 2 kA and a duration of 100 ns. Moreover, it was found that the diode electron current is many times the Child – Langmuir current and that it increases still further if the cathode – anode gap is preliminarily filled with plasma, the amount of the increase depending on how much the pulse fed to the substrate overtakes the anode voltage pulse. With such a cathode, a high-current pulsed electron accelerator with an energy of 550 kV, a current of 10 kA, and a pulse duration of 25 ns was built.

The reason for using a ferroelectric as the dielectric in the proposed cathode concept is its large dielectric constant ($\varepsilon > 10^3$), which results in both the normal, E_n, and the tangential, E_t, electric fields in the gap of the metal – dielectric contact increasing sharply compared to those for usual ($\varepsilon < 10$) ceramics ($E_n \sim \varepsilon$, and $E_t \sim \varepsilon^{1/2}$). This leads to more intense surface discharge processes in TJs of the first type — that is, in those with cathode microprotrusions touching the dielectric. In TJs of the second type, where microprotrusions do not touch but hang over the dielectric, charged-particle emission processes are intensified. The fluxes of charged particles bombard the dielectric and initiate a surface discharge, on the one hand, and heat it up, on the other, and when their current density exceeds a certain critical value, the surface of the ceramics explodes, giving rise to plasma that contains the atoms and ions of the ceramic material. All this combined sharply reduces the amplitude of the triggering pulse applied to the substrate. Thus, the participation of surface discharge plasma was from the outset a feature of the very idea of the ferroelectric cathode.

However, starting from 1988, the idea, first suggested at CERN, has been actively developed at many laboratories in the US, Europe, and Japan that this emission occurs directly from the surface of the ferroelectric which has the ability to change initial polarization when subjected to a high-voltage pulse. It was believed that the nanosecond inversion of polarization of domains in the ferroelectric induces an electric field of up to 10^9 V cm^{-1} and leads to the formation near the ferroelectric surface of an uncompensated negative charge from 'free' electrons and domain charges. This results in strong field emission from the ferroelectric surface. Such a process was termed ferroemission. Although this physical interpretation was inconsistent with experiments yet to be done (which decisively indicated the fundamental role of triple junctions and plasma at the cathode), it was this interpretation which in the 1980s – 1990s and at the beginning of this century prompted a flurry of theoretical, experimental, and design research on ferroelectric-based cathodes, with a view to developing a novel, solid-state, nonincandescent cathode to replace the thermionic one.

To conclusively prove the role of TJs and plasma in the operation of these cathodes, the present author and his coworkers carried out a series of experiments with point cathodes. In this case, a sharp needle pressed to the (grounded) surface of the dielectric was used instead of the grid. When a substrate located at the opposite side of the ferroelectric plate was subjected to a voltage pulse $10^{-9} - 10^{-8}$ s in duration, a plasma glow was observed on the ferroelectric around the needle, with the plasma extending at a speed v_d of about 10^7 cm s^{-1}. The spectrum of the glow showed the atomic and ion spectral lines of both the needle metal and ceramic material. With a voltage across the substrate of 1 to 3 kV, the bias current due to the surface discharge amounted to 1 – 10 A. The energy release in such a discharge reached a value of around 10^{-3} J. The electron current from the point cathode at a voltage of 25 kV at the anode was 5 – 15 A. If the triggering voltage pulse arrived no later than the accelerating one, then the ratio of the electron current emitted by the needle in the presence of the ferroelectric to the current in its absence (i.e., to the current of explosive emission) was $\sim v_d/v$, where v is the velocity of the explosive emission plasma. If the triggering pulse was leading, the electron current was considerably larger and exceeded the Child – Langmuir value. It is shown that in the nanosecond duration range electron emission from a point cathode results from explosive emission from the contact, due to cathode microprotrusions being Joule-heated by the bias current. Evidence for this includes the motion of the plasma toward the anode at a velocity of around 10^6 cm s^{-1}, electron current spikes, the spectral lines of the excited atoms and ions of the cathode metal in the spectrum, etc. Note that the bias current $i_f \sim \varepsilon$ and that the delay time of its explosion is $t_d \sim \varepsilon^{-2}$. All the data obtained for the point cathode showed that plasma plays a fundamental role in its operation. The results with a barium – titanate-based point cathode turned out to be, in principle, the same as for planar cathodes with metal grids and PLZT and PZT ferroelectrics. In particular, the electron current exceeded the Child – Langmuir limit, the plasma radiation spectrum showed the spectral lines of the grid metal and those of the elements of the ceramics, plasma flows contained ions with a velocity of $\sim 10^6$ cm s^{-1}, etc. What all this implies is that in the grid cathode there are a large number of TJs in the grid – ferroelectric contact. There are, however, differences in how these cathodes operate. First, plasma in the grid cathode turned out to be on average an order of magnitude slower than that in the point cathode. Second, in the point cathode all cathode processes were more intense at a positive rather than at a negative needle-to-substrate polarity, whereas in the grid cathode all processes at the cathode and in the diode were more intense at a positive grid.

Thus, it can be considered a proven fact that the so-called ferroelectric cathodes fundamentally rely on plasma processes. For this reason, such cathodes should be called

ferroelectric plasma (FEP) cathodes. A key factor affecting their operation is the large value of the dielectric constant.

Electrons in such cathodes are not emitted from the surface of the ferroelectric but from the metal of the grid, and there are two mechanisms by which they are extracted. One of these, explosive emission, undoubtedly occurs in the nanosecond range ($10^{-9}-10^{-8}$ s). The second is secondary electron emission due to the cathode being bombarded by positive plasma ions (as in conventional plasma cathodes); this kind of emission occurs in the microsecond range of electron flow durations, although explosive electron emission initiated by plasma is also present in this range. It is this plasma which makes the electron current in the FEP cathode self-sustained.

Practical applications of FEP cathodes are implemented through the use of an additional grid, whose role is to make the electron beam more uniform. Such grid cathodes originally found wide application in plasma electron sources based on various types of discharges (arc, glow discharge, hollow cathode, etc.). FEP cathodes are already used in electron accelerators, microwave oscillators, masers, free electron lasers, triggering systems of high-power gas switches, etc., occupying a niche between thermionic and explosive electron emission cathodes. Although there is much work still to be done to improve their service life and vacuum-proof performance and to reduce the effect of ion flows on the electron beam parameters, the diodes with such cathodes have many useful and nice features, such as: the simple control of electron beam parameters by varying the trigger voltage pulse's time delay; an electron current well above the Child – Langmuir limit; electron beams produced over a wide range of durations ($10^{-9}-10^{-3}$ s) and in a technical vacuum, and, finally, outstanding ease of fabrication and operation.

Acknowledgments

The author thanks I I Ivanchik, V G Shpak, and N V Gavrilov for the very fruitful discussions of parts of this paper.

References

1. Mesyats G A *Impul'snaya Energetika i Elektronika* (Pulsed Power and Electronics) (Moscow: Nauka, 2004) [Translated into English: *Pulsed Power* (New York: Kluwer Acad./Plenum Publ., 2005)]
2. Mesyats G A "Issledovaniya po generirovaniyu nanosekundnykh impul'sov bol'shoi moshchnosti" ("Research into the generation of high power nanosecond pulses"), Thesis for Doctorate of Technical Sciences (Tomsk: Tomskii Politekh. Inst., 1966)
3. Bugaev S P, Mesyats G A *Zh. Tekh. Fiz.* **37** 1861 (1967) [*Sov. Phys. Tech. Phys.* **12** 1363 (1968)]
4. Bugaev S P, Koval'chuk B M, Mesyats G A "Plazmennyi impul'snyi istochnik zaryazhennykh chastits" ("Plasma-based pulsed source of charged particles"), USSR Author's Certificate No. 24809 (appl. 05.11.67); *Otkrytiya, Izobret. Prom. Obraztsy, Tovar. Znaki* **45** 231 (1973)
5. Bugaev S P, Zagulov F Ya, Koval'chuk B M, Mesyats G A *Izv. Vyssh. Uchebn. Zaved. Fiz.* (1) 145 (1968) [*Sov. Phys. J.* **11** 89 (1968)]
6. Rosenman G et al. *J. Appl. Phys.* **88** 6109 (2000)
7. Riege H *Nucl. Instrum. Methods Phys. Res. A* **340** 80 (1994)
8. Rosenman G, Rez I *J. Appl. Phys.* **73** 1904 (1993)
9. Ivers J D et al. *J. Appl. Phys.* **73** 2667 (1993)
10. Merz W J *Phys. Rev.* **95** 690 (1954)
11. Gundel H, in *Science and Technology of Electroceramic Thin Films: Proc. NATO Advanced Research Workshop* (NATO ASI Series, Ser. E, Vol. 284, Eds O Auciello, R Waser) (Dordrecht: Kluwer Acad., 1995) p. 335
12. Stadler H L, Zachmanidis P J *J. Appl. Phys.* **34** 3255 (1963)
13. Kang B-S, Gu-Choi D, Choi S-K *J. Mater Sci.: Mater. Electron.* **9** 139 (1998)
14. Rosenman G et al. *J. Appl. Phys.* **82** 772 (1997)
15. Shur D et al. *J. Appl. Phys.* **79** 3669 (1996)
16. Benedek G et al. *J. Appl. Phys.* **81** 1396 (1997)
17. Okuayma M, Asano J, Hamakawa Y *Jpn. J. Appl. Phys.* **33** 5506 (1994)
18. Asano J, Okuyama M, Hamakawa Y *Jpn. J. Appl. Phys.* **32** 396 (1993)
19. Kugel V D et al. *J. Appl. Phys.* **78** 2248 (1995)
20. Shur D, Rosenman G, Krasik Ya E *Appl. Phys. Lett.* **70** 574 (1997)
21. Zhang W et al. *J. Appl. Phys.* **83** 6055 (1998)
22. Shannon D N J et al. *Appl. Phys. Lett.* **70** 1625 (1997)
23. Skanavi G I *Fizika Dielektrikov* (*Oblast' Sil'nykh Polei*) [Physics of Dielectrics (Strong-Field Range)] (Moscow: GIFML, 1958)
24. Mesyats G A, Proskurovsky D I *Impul'snyi Elektricheskii Razryad v Vakuume* (Pulsed Electrical Discharge in Vacuum) (Novosibirsk: Nauka, 1984) [Translated into English (Berlin: Springer-Verlag, 1989)]
25. Kofoid M J *AIEE Trans. Power Apparat. Syst.* **79** 991 (1960)
26. Mesyats G A, Proskurovskii D I *Pis'ma Zh. Eksp. Teor. Fiz.* **13** 7 (1971) [*JETP Lett.* **13** 4 (1971)]
27. Mesyats G A *Ektony v Vakuumnom Razryade: Proboi, Iskra, Duga* (Cathode Phenomena in a Vacuum Discharge: the Breakdown, the Spark, and the Arc) (Moscow: Nauka, 2000) [Translated into English (Moscow: Nauka Publ., 2000)]
28. Shrednik V N, in *Nenakalivaemye Katody* (Non-Incandescent Cathodes) (Ed. M I Elinson) (Moscow: Sov. Radio, 1974) p. 165
29. Mesyats G A *Pis'ma Zh. Eksp. Teor. Fiz.* **57** 88 (1993) [*JETP Lett.* **57** 95 (1993)]
30. Bazhenov G P, Rotshtein V P, in *Moshchnye Nanosekundnye Impul'snye Istochniki Uskorennykh Elektronov* (High-Power Pulsed Nanosecond Sources of Accelerating Electrons) (Executive Ed. G A Mesyats) (Novosibirsk: Nauka, 1974) p. 67
31. Bugaev S P, Mesyats G A *Dokl. Akad. Nauk SSSR* **196** 324 (1971) [*Sov. Phys. Dokl.* **16** 41 (1971)]
32. Bugaev S P, Shpak V G, in *Moshchnye Nanosekundnye Impul'snye Istochniki Uskorennykh Elektronov* (High-Power Pulsed Nanosecond Sources of Accelerating Electrons) (Executive Ed. G A Mesyats) (Novosibirsk: Nauka, 1974) p. 71
33. Shpak V G *Izv. Vyssh. Uchebn. Zaved. Fiz.* (4) 131 (1975) [*Sov. Phys. J.* **18** 563 (1975)]
34. Shpak V G "Generirovanie moshchnykh subnanosekundnykh elektronnykh puchkov" ("Generation of high-power subnanosecond electron beams"), Thesis for Candidate of Technical Sciences (Tomsk: Tomskii Inst. Avtomatizir. Sistem Upravleniya i Radioelektroniki, 1980)
35. Mesyats G A *Dokl. Ross. Akad. Nauk* **336** 610 (1994) [*Phys. Dokl.* **39** 417 (1994)]
36. Bugaev S P et al. *Zh. Tekh. Fiz.* **41** 1958 (1971) [*Sov. Phys. Tech. Phys.* **16** 1547 (1971)]
37. Bugaev S P, Mesyats G A, in *Impul'snyi Razryad v Dielektrikakh* (Pulsed Discharge in Dielectrics) (Executive Ed. G A Mesyats) (Novosibirsk: Nauka, 1985) p. 4
38. Borovik E S, Batrakov B P *Zh. Tekh. Fiz.* **28** 1621 (1958)
39. Gleichauf P H *J. Appl. Phys.* **22** 535 (1955)
40. Thompson J E et al. *IEEE Trans. Plasma Sci.* **8** 191 (1980)
41. Mesyats G A *Explosive Electron Emission* (Ekaterinburg: URO-Press, 1998)
42. Gundel H, Hańderek J, Riege H *J. Appl. Phys.* **69** 975 (1991)
43. Asano J et al. *Jpn. J. Appl. Phys.* **31** 3098 (1992)
44. Cavazos T C et al. *Appl. Phys. Lett.* **65** 2612 (1994)
45. Sampayan S E et al. *Nucl. Instrum. Methods Phys. Res. A* **340** 90 (1994)
46. Airapetov A Sh et al. *Dokl. Akad. Nauk SSSR* **311** 594 (1990) [*Sov. Phys. Dokl.* **35** 267 (1990)]
47. Zhang W, Huebner W *J. Appl. Phys.* **83** 6034 (1998)
48. Mesyats G A *Generirovanie Moshchnykh Nanosekundnykh Impul'sov* (Generation of High-Power Nanosecond Pulses) (Moscow: Sov. Radio, 1974)
49. Dunaevsky A et al. *J. Appl. Phys.* **85** 8464 (1999)
50. Boscolo I, Scurati A, Stellato M *J. Appl. Phys.* **85** 8337 (1999)
51. Mesyats G A, in *XVI Intern. Symp. on Discharges and Electrical Insulation in Vacuum, Moscow – St. Petersburg, Russia, 29 – 30 May*

1994 (Proc. SPIE, Vol. 2259, Ed. G A Mesyats) (Bellingham, Wash.: SPIE, 1994) p. 419
52. Auciello O et al. *Appl. Phys. Lett.* **66** 2183 (1995)
53. Jiang B, Kirkman G, Reinhardt N *Appl. Phys. Lett.* **66** 1196 (1995)
54. Riege H et al. *J. Appl. Phys.* **84** 1602 (1998)
55. Mesyats G A *IEEE Trans. Dielectr. Electr. Insul.* **2** 272 (1995)
56. Gundel H et al. *Ferroelectrics* **100** 1 (1989)
57. Flechtner D et al. *J. Appl. Phys.* **83** 955 (1998)
58. Shur D et al. *J. Phys. D: Appl. Phys.* **31** 1375 (1998)
59. Dunaevsky A et al. *J. Appl. Phys.* **85** 8474 (1999)
60. Kreindel' Yu E *Plazmennye Istochniki Elektronov* (Plasma Electron Sources) (Moscow: Atomizdat, 1977)
61. Oks E M *Istochniki Elektronov s Plazmennym Katodom: Fizika, Tekhnika, Primeneniya* (Plasma Cathode Electron Sources: Physics, Technology, Applications) (Tomsk: Izd. Nauchno-Tekh. Lit., 2005) [Translated into English (Weinheim: Wiley-VCH, 2006)]
62. Bugaev S P et al. *Prib. Tekh. Eksp.* (6) 15 (1970) [*Instrum. Exp. Tech.* (6) 1557 (1970)]
63. Mendel C W (Jr.), Goldstein S A *J. Appl. Phys.* **48** 1004 (1977)
64. Kreindel M Yu et al. *Fiz. Plazmy* **17** 1425 (1991) [*Sov. J. Plasma Phys.* **17** 825 (1991)]
65. Gundel H et al., CERN/PS/88-66 (AR)
66. Gundel H et al. *Appl. Phys. Lett.* **54** 2071 (1989)
67. Gundel H et al. *Ferroelectrics* **110** 183 (1990)
68. Averty D, Liateni S F, Le Bihan R *Ferroelectrics* **173** 171 (1995)
69. Krasik Ya E, Dunaevsky A, Felsteiner J *J. Appl. Phys.* **85** 7946 (1999)
70. Gundel H et al. *Nucl. Instrum. Methods Phys. Res. A* **340** 102 (1994)
71. Shur D, Rosenman G *J. Phys. D: Appl. Phys.* **32** L29 (1999)
72. Mesyats G A, Nasibov A S, Kremnev V V *Formirovanie Nanosekundnykh Impul'sov Vysokogo Napryazheniya* (Formation of High-Voltage Nanosecond Pulses) (Moscow: Energiya, 1970)
73. Ready J F *Industrial Applications of Lasers* (New York: Academic Press, 1978)
74. Puchkarev V F, Mesyats G A *J. Appl. Phys.* **78** 5633 (1995)
75. Mesyats G A *Pis'ma Zh. Tekh. Fiz.* **20** 17 (1994) [*Tech. Phys. Lett.* **20** 8 (1994)]
76. Geissler K et al. *Phys. Lett. A* **166** 84 (1992)
77. Fatuzzo E, Merz W J *Ferroelectricity* (Amsterdam: North-Holland, 1967)
78. Jona F, Shirane G *Ferroelectric Crystals* (Oxford: Pergamon Press, 1962)
79. Riege H et al. *Bull. Am. Phys. Soc.* **34** 193 (1989)
80. Advani R N et al. *IEEE Trans. Plasma Sci.* **26** 1347 (1998)
81. Hershcovitch A *Appl. Phys. Lett.* **68** 464 (1996)
82. Pleyber G, Biedrzycki K, Le Bihan R *Ferroelectrics* **141** 125 (1993)
83. Vaisburd D I, Mesyats G A *Vestn. Akad. Nauk SSSR* (1) 62 (1983)
84. Ivers J D et al. *IEEE Trans. Plasma Sci.* **27** 707 (1999)
85. Thumm M *Appl. Surf. Sci.* **111** 106 (1997)
86. Drori R et al. *Appl. Phys. Lett.* **74** 335 (1999)
87. Shahadi A et al. *Nucl. Instrum. Methods Phys. Res. A* **375** 140 (1996)
88. Bergmann K et al. *Appl. Phys. Lett.* **71** 1936 (1997)
89. Krasik Ya E, Dunaevsky A, Felsteiner J *Appl. Phys. Lett.* **73** 453 (1998)
90. Dunaevsky A et al. *J. Appl. Phys.* **86** 4107 (1999)
91. Krokhmal A et al. *J. Appl. Phys.* **94** 44 (2003)
92. Krokhmal A et al. *J. Appl. Phys.* **95** 3304 (2004)
93. Gavrilov N V, Kreindel Yu E, Mesyats G A, Shvedov F N *Pis'ma Zh. Tekh. Fiz.* **14** 865 (1988) [*Sov. Tech. Phys. Lett.* **14** 383 (1988)]
94. Zlobina A F et al. *Zh. Tekh. Fiz.* **50** 1203 (1980) [*Sov. Phys. Tech. Phys.* **25** 689 (1980)]
95. Zharinov A V et al. *Zh. Tekh. Fiz.* **56** 66 (1986) [*Sov. Phys. Tech. Phys.* **31** 39 (1986)]
96. Zharinov A V et al. *Zh. Tekh. Fiz.* **57** 877 (1987) [*Sov. Phys. Tech. Phys.* **32** 533 (1987)]
97. Koval N N, Kreindel Yu E, Shanin P M *Zh. Tekh. Fiz.* **53** 1846 (1983) [*Sov. Phys. Tech. Phys.* **28** 1133 (1983)]
98. Metel A S et al. *Zh. Tekh. Fiz.* **54** 241 (1984) [*Sov. Phys. Tech. Phys.* **29** 141 (1984)]
99. Gleizer J Z et al. *Eur. Phys. J. D* **26** 285 (2003)
100. Krokhmal A et al. *J. Appl. Phys.* **94** 55 (2003)
101. Gleizer J Z et al. *J. Phys. D: Appl. Phys.* **38** 276 (2005)